

Hypercongestion, autonomous vehicle, and urban spatial structure

Takao Dantsuji^{*†} Yuki Takayama[‡]

Abstract

This paper examines the effects of hypercongestion mitigation by perimeter control and the introduction of autonomous vehicles on the spatial structures of cities. By incorporating a bathtub model, we develop a land use model where hypercongestion occurs in the downtown area and interacts with land use. We show that hypercongestion mitigation by perimeter control decreases the commuting cost in the short-run and results in a less dense urban spatial structure in the long-run. Furthermore, we reveal that the impact of autonomous vehicles depends on the presence of hypercongestion. Introduction of autonomous vehicles may increase the commuting cost in the presence of hypercongestion and cause a decrease in suburban population, but make cities spatially expanded outward. This result contradicts that of the standard bottleneck model. When perimeter control is implemented, the introduction of autonomous vehicles decreases the commuting cost and results in a less dense urban spatial structure. These results show that hypercongestion is a key factor that can change urban spatial structures.

Keywords: hypercongestion; perimeter control; autonomous vehicle; bathtub model; land use model.

1 Introduction

1.1 Background

Traffic demand is highly concentrated during rush hours in urban cities, which causes hypercongestion (the downward-sloping part of the inverted U-shaped relationship between traffic flow and traffic density), and dispersing traffic demand can change the spatial distribution of residents in the long-run. Recent research has shown that downtown areas experience network-wide hypercongestion (e.g., Daganzo, 2007; Geroliminis and Daganzo, 2008) and that the temporal concentration of traffic demand leads to network *capacity drop* (e.g., Small and Chu, 2003; Geroliminis and Levinson, 2009; Arnott, 2013). Capacity drop is phenomenon where throughput (e.g., flow or outflow) decreases with an increase in the number of vehicles circulating in networks.

A number of studies have proposed traffic demand management (TDM) strategies, such as congestion pricing (e.g., Geroliminis and Levinson, 2009) and perimeter control (e.g., Haddad and Geroliminis, 2012; Tsekeris and Geroliminis, 2013), to disperse traffic demand during peak periods for hypercongestion mitigation as capacity drop causes the inefficient use of transportation systems. However, most of them focused on problems under the assumption that commuters do not relocate (i.e., fixed origin-destination

^{*}Monash Institute of Transport Studies, Monash University, 23 College Walk, Clayton, Victoria 3800, Australia
Takao.Dantsuji@monash.edu

[†]Institute of Science and Engineering, Kanazawa University, Kakuma-machi, Kanazawa, Ishikawa 920-1192, Japan

[‡]Department of Civil and Environmental Engineering, Tokyo Institute of Technology, 2-12-1 W6-9, Ookayama, Meguro, Tokyo 152-8550, Japan, takayama.y.af@m.titech.ac.jp

demand). That is, they ignored changes in residents’ spatial distribution in response to their commuting behavior changes and instead focused on the short-run effects of TDM strategies. Since commuting and land use patterns influence each other substantially (Kanemoto, 1980), the long-run impacts of TDM strategies on land use should be understood to promote efficient and sustainable urban developments.

Models of urban spatial structures can describe the interaction between commuting and residential locations (Alonso, 1964). Traditional models that employ static congestion models (e.g., Anas et al., 1998) have been extended to incorporate dynamic bottleneck congestion (e.g., Arnott, 1998; Gubins and Verhoef, 2014; Takayama and Kuwahara, 2017; Fosgerau et al., 2018; Xu et al., 2018; Fosgerau and Kim, 2019; Takayama, 2020; Li et al., 2023). These extended models highlight the significance of the temporal distribution of traffic demand and dynamic congestion phenomena in long-run equilibrium; however, they cannot incorporate hypercongestion, where capacity can drop over time, unlike in bottleneck congestion. A suitable model is yet to be developed to examine the long-run effectiveness of TDM strategies for hypercongestion mitigation. Furthermore, whether hypercongestion is a key factor that can alter urban spatial structures remains an open question in the literature.

In this new era of autonomous vehicles, hypercongestion can play a more important role in TDM strategies. According to van den Berg and Verhoef (2016), autonomous vehicle can enhance network capacity because they safely drive closer to each other than vehicles driven by humans (“Network capacity” effect hereafter), and passengers in autonomous vehicles are less concerned about travel times because they do not need to drive anymore (“VOT effect” hereafter). van den Berg and Verhoef (2016) showed that both network capacity and VOT effects decrease the commuting cost in fully automated traffic bottleneck congestion. Furthermore, existing works (e.g., Lu et al., 2020; Moshahedi and Kattan, 2022) demonstrated the network flow can be enhanced by the network capacity effect. However, the VOT effect on network efficiency has been insufficiently studied because it is not as simple as the network capacity effect. The VOT effect reduces the the cost of travel time; however, an increase in the VOT effect is expected to worsen capacity drop due to the temporal concentration of traffic demand. Thus, traffic demand patterns with autonomous vehicles will become increasingly complex in the presence of hypercongestion. A model that systematically analyzes these impacts on the temporal and spatial distributions of traffic demand should be developed to investigate the long-run effects of TDM strategies in this new era of autonomous vehicles properly.

In this paper, by incorporating a bathtub model, we develop a land use model where hypercongestion occurs in the downtown area and interacts with land use. Our findings show that the implementation of perimeter control for hypercongestion mitigation decreases the commuting cost, and results in a less dense urban spatial structure. Furthermore, we find that the use of autonomous vehicles may increase the commuting cost due to the severe capacity drop caused by the temporal concentration of traffic demand, and cause an increase in downtown population, but make cities spatially expanded outward. This result contradicts that of the standard bottleneck model. When perimeter control is implemented, the introduction of autonomous vehicles decreases the commuting cost, and results in a less dense urban spatial structure. These results show that hypercongestion is a key factor that can change urban spatial structures.

1.2 Literature Review

Network-wide hypercongestion, namely Macroscopic Fundamental Diagrams (MFDs) is a powerful tool for describing network-wide traffic dynamics; this approach relates network flow (or trip completion rate) to network density (or accumulation of vehicles). The idea of macroscopic traffic theory was proposed

by Godfrey (1969), further investigated by Daganzo (2007), and empirically analyzed by Geroliminis and Daganzo (2008). Traffic management approaches based on MFDs have been studied, such as pricing (e.g., Zheng et al., 2012; Simoni et al., 2015; Dantsuji et al., 2021; Genser and Kouvelas, 2022), perimeter control (e.g., Daganzo, 2007; Tsekeris and Geroliminis, 2013; Haddad and Shraiber, 2014), route guidance (e.g., Yildirimoglu et al., 2015, 2018), and road space allocation (e.g., Zheng and Geroliminis, 2013; Chiabaut, 2015; Zheng et al., 2017). MFDs have also been utilized for other purposes, such as dynamic traffic demand estimation (e.g., Dantsuji et al., 2022) and network performance indication (e.g., Loder et al., 2019).

Perimeter control is a successful application of MFDs in TDM strategies as an effective and easy-to-implement tool. It aims to control the entry flow at the perimeter boundary of a target area to maximize the trip completion rate. This approach has been extended to multiregion networks (e.g., Geroliminis et al., 2012; Haddad and Geroliminis, 2012; Ramezani et al., 2015; Haddad and Zheng, 2020; Sirmatel et al., 2021; Fu et al., 2021; Batista et al., 2021; Zhou and Gayah, 2023; Chen et al., 2022a; Kouvelas et al., 2023), perimeter control with boundary queues (e.g., Haddad, 2017; Ni and Cassidy, 2020; Guo and Ban, 2020; Li et al., 2021) and route guidance (e.g., Sirmatel and Geroliminis, 2017; Ding et al., 2017; Fu et al., 2021), and bimodal transportation systems (e.g., Ampountolas et al., 2017; Haitao et al., 2019; Chen et al., 2022b; Dantsuji et al., 2023). Considerable effort has been dedicated to perimeter control schemes, but there are no studies that examined the impacts of autonomous vehicles (i.e., VOT and network capacity effects) on their effectiveness. Furthermore, despite the significant influence of perimeter control on traffic demand, most of the studies made the assumption that origin-destination demand is fixed. This hinders a comprehensive understanding of the interplay between urban and transportation developments. A critical gap is the lack of a methodology that connects short-run commuters' decisions (e.g., trip timing) with their residential location choices in the long-run.

Traditional land use models that consider the trade-off between land rent and commuting costs in a monocentric city effectively analyze residential location patterns. Static congestion models (e.g., Kanemoto, 1980; Anas et al., 1998) have been extended to dynamic bottleneck models (Arnott, 1998) to incorporate the impact of the trip timing decisions of commuters into their residential location choices in the long-run. Several aspects have been incorporated into the standard bottleneck model as extensions, such as an incentive for commuters to spend time at home (Gubins and Verhoef, 2014), bimodal transportation systems (Xu et al., 2018), an open city model (Fosgerau et al., 2018), a tandem bottlenecks (Fosgerau and Kim, 2019), a bottleneck with a stochastic location (Li et al., 2023), and commuters' heterogeneity (Takayama and Kuwahara, 2017; Takayama, 2020). These aspects can alter urban spatial structures in the long-run, but whether hypercongestion has the same effect remains an open question in the literature.

The trip timing decisions of commuters in the presence of hypercongestion can be described using bathtub models, namely dynamic user equilibrium models for departure time choices in urban cities with hypercongestion (e.g., Small and Chu, 2003; Geroliminis and Levinson, 2009; Arnott, 2013; Fosgerau and Small, 2013; Vickrey, 2020; Bao et al., 2021; Ameli et al., 2022). Bathtub models have been extended to trip length heterogeneity (e.g., Fosgerau and Small, 2013; Lamotte and Geroliminis, 2018), cruising-for-parking (e.g., Geroliminis, 2015; Liu and Geroliminis, 2016), and bimodal transportation systems (e.g., Gonzales and Daganzo, 2012; Gonzales, 2015; Dantsuji et al., 2023). However, none of them considered changes in residents' spatial distribution in response to their commuting behavior changes.

Our recent work (Dantsuji et al., 2023) developed the bimodal bathtub model, and investigated the travelers' behavior changes in response to perimeter control with transit priority. However, they focused only on the short-run equilibrium. How to combine the short-run equilibrium in the presence of

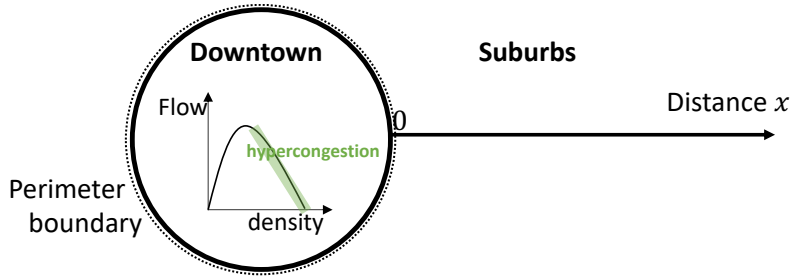


Figure 1: Model structure

hypercongestion with the long-run equilibrium remains a challenging topic. Also, Dantsuji et al. (2023) did not consider the impacts of autonomous vehicles. While there are a vast of literature on the network capacity and VOT effects of autonomous vehicles, no one proves that the VOT effect may cause higher commuting cost in the presence of hypercongestion. To the best of our knowledge, our study is the first to systematically analyze a model in which commuters choose their trip timing in the presence of hypercongestion in the short-run and residential location in the long-run.

The remaining of this paper is organized as follows. Section 2 shows the development of the model. Section 3, we characterize the model equilibrium. Section 4 presents the formulation of the model during perimeter control. The equilibrium conditions during perimeter control are studied in Section 5. Numerical examples are provided in Section 6, and we conclude this paper in Section 7.

2 Model

Consider a monocentric city that has downtown and suburban areas. All job opportunities are found and homogeneously distributed in the downtown area, whereas there are residential areas in both downtown and suburban areas. The downtown area is in the center of the city, and a residential location in the suburban area is indexed by a distance x from the edge of the downtown area (Fig 1). The areas of downtown and suburban at location x have fixed land areas of A_d and $A_s(x)$, respectively. We assume that the land is owned by absentee landlords, as is common in the literature. An N continuum of homogeneous commuters have identical preferences and the numbers of downtown commuters and suburban commuters at location x are denoted by N_d and $N_s(x)$, respectively.

2.1 Hypercongestion and commuting cost

The downtown area has homogeneous topological characteristics by proper partitioning approaches (e.g., Ji and Geroliminis, 2012; Dantsuji et al., 2020), thus showing a well-defined relationship between space-mean flow and density. Note that as we assume that the job opportunities are homogeneously distributed in the downtown area, the shape of the MFD does not change even when commuters' residential locations change. The congestion dynamics in the downtown area are described using a bathtub model, whereas we assume that one can travel at a free-flow speed in the suburban area. To incorporate hypercongestion, we employ the Greenshields model for the space-mean speed as follows.

$$v(t) = v_f \left(1 - \frac{n(t)}{n_j} \right), \quad (1)$$

where $v(t)$ is the space-mean speed at time t , v_f is the free-flow speed, $n(t)$ is the vehicle accumulation in the downtown area at time t and n_j is jam accumulation.

Since the downtown area is modeled as a system with inflows and outflows and whose traffic conditions are governed by bathtub congestion dynamics, the time evolution of vehicle accumulation, $\dot{n}(t)$, is

$$\dot{n}(t) = I(t) - G(t), \quad (2)$$

where $I(t)$ is the inflow and $G(t)$ is the outflow at time t . The outflow is formulated using the network exit function (NEF) as follows:

$$G(t) = \frac{n(t)v(t)}{L}, \quad (3)$$

where L is the average trip length in the downtown area.

The travel time in the downtown area is assumed to be determined by a single instant of time for tractability (Small and Chu, 2003; Geroliminis and Levinson, 2009) and calculated as

$$T(t) \approx \frac{L}{v(t)}. \quad (4)$$

All suburban commuters have identical trip lengths L in the downtown area.

This instantaneous travel time assumption is based on the so-called accumulation-based modelling, where the outflow is a function of the instantaneous accumulation (Mariotte et al., 2017). According to Mariotte et al. (2017), in cases where the inflow changes drastically over time, information propagates too fast, which leads to a physical inconsistency. An alternative approach is the trip-based model (e.g., Fosgerau, 2015; Mariotte et al., 2017; Lamotte and Geroliminis, 2018; Jin, 2020), which can tackle this inconsistency. However, the trip-based model is typically intractable. Even though the inconsistency occurs at the beginning and end of the rush hour when the inflow changes drastically, it does not affect the qualitative results in this paper. Therefore, we employ the accumulation-based model for tractability.

We assume that the downtown commuters commute by walking or cycling and the suburban commuters travel by car, which is similar to the modeling of Arnott (1998). The commuting cost of a downtown commuter and a suburban commuter at location x who arrive at work at time t ($C_d(t)$ and $C_s(x, t)$, respectively) are expressed as

$$C_d(t) = \alpha T_d + s(t), \quad (5a)$$

$$C_s(x, t) = \alpha (T(t) + \tau x) + s(t), \quad (5b)$$

$$s(t) = \begin{cases} \beta (t^* - t) & \text{if } t \leq t^* \\ \gamma (t - t^*) & \text{if } t > t^* \end{cases}, \quad (5c)$$

where T_d represents the constant travel time of the downtown commuters, $T(t)$ represents the travel time in the downtown area at time t , τx represents the suburban free-flow travel time of commuters residing at x (i.e., $\tau = 1/v_f$), t^* represents the desired arrival time, and α , β and γ are marginal costs of travel time, earliness, and lateness. The first and second terms on the RHS of Eq. (5b) are the travel time cost and schedule delay cost, respectively. That is, we assume that commuters have “ α - β - γ ” type preference (Arnott et al., 1993).

We also consider a situation where every vehicle is an autonomous vehicle. Autonomous vehicles are expected to have two effects: the VOT effect and the network capacity effect (van den Berg and Verhoef, 2016). In this study, the former effect is represented by a reduction in the VOT. It is $\eta\alpha$ where η is the VOT effect parameter ($\frac{\beta}{\alpha} < \eta \leq 1$). The latter effect is captured by an increase in network capacity, which is ξn_j where ξ is the network capacity effect parameter ($\xi \geq 1$). This effect increases not only the network capacity but also the critical accumulation, which is consistent with the simulation analysis by Lu et al. (2020).

There is a large literature on the VOT effect since it can be estimated by stated preference surveys. Steck et al. (2018) found privately owned autonomous vehicle reduces value of travel time savings (VTTS) by 31 %. Zhong et al. (2020) investigated the VOT effects in suburban, urban, and rural areas, and found 24 % decrease in the urban area. de Almeida Correia et al. (2019) and Kolarova and Cherchi (2021) found 26 % and 41 % VTTS reduction, respectively. The range of the VOT effect is from 24 % to 41 %.

As van den Berg and Verhoef (2016) indicated, the network capacity effect is still an open question in literature. The literature showed that an increase in capacity ranges from 1 % to 414 % (see Table 1 in van den Berg and Verhoef (2016)). At network level, Lu et al. (2020) showed that the network capacity increases by 16 % and Moshahedi and Kattan (2022) found the enhancement of 30 % in the outflow. However, these studies do not use the real dataset. Huang et al. (2023) found the network capacity effect ranging from 2.9 % to 19 % through simulation analysis calibrated by public autonomous vehicle datasets.

2.2 Commuter preferences

We next incorporate the commuting cost in the presence of hypercongestion into commuter preferences. The utility of downtown commuters is expressed as the following Cobb–Douglas utility function:

$$u_d(z_d(t), a_d(t)) = \{z_d(t)\}^{1-\mu} \{a_d(t)\}^\mu, \quad (6)$$

where $\mu \in (0, 1)$, $z_d(t)$ represents the consumption of the numéraire good and $a_d(t)$ represents the lot size of housing which downtown commuters consume. The budget constraint is

$$w = z_d(t) + (r_d + r_A)a_d(t) + C_d(t), \quad (7)$$

where w represents their income, $r_A > 0$ represents the exogenous agricultural rent, and $r_d + r_A$ represents the downtown land rent. The first-order conditions of the utility maximization problem are

$$z_d(t) = (1 - \mu) y_d(t), \quad (8a)$$

$$a_d(t) = \frac{\mu y_d(t)}{r_d + r_A}, \quad (8b)$$

$$y_d(t) = w - c_d(t), \quad (8c)$$

where $y_d(t)$ represents the income net of commuting cost earned by a downtown commuter who arrives at work at time t . Substituting this into the utility function, we obtain the indirect utility function as

$$U_d(y_d(t), r_d + r_A) = (1 - \mu)^{1-\mu} \mu^\mu y_d(t) (r_d + r_A)^{-\mu}. \quad (9)$$

Similarly, we formulate a land use model for the suburban commuters. Their utility and budget constraint are respectively expressed as

$$u_s(z_s(x, t), a_s(x, t)) = \{z_s(x, t)\}^{1-\mu} \{a_s(x, t)\}^\mu, \quad (10)$$

$$w = z_s(x, t) + (r_s(x) + r_A)a_s(x, t) + C_s(x, t), \quad (11)$$

where $z_s(x, t)$ represents the consumption of the numéraire good, $a_s(x, t)$ represents the lot size of housing consumed by the suburban commuters at x , and $r_s(x) + r_A$ represents the land rent at x . Then, the first-order conditions of the utility maximization problem are

$$z_s(x, t) = (1 - \mu) y_s(x, t), \quad (12a)$$

$$a_s(x, t) = \frac{\mu y_s(x, t)}{r_s(x) + r_A}, \quad (12b)$$

$$y_s(x, t) = w - c_s(x, t), \quad (12c)$$

where $y_s(x, t)$ represents the income net of commuting cost earned by a commuter who resides at x and arrives at work at time t . The indirect utility function is

$$U_s(y_s(x, t), r_s(x) + r_A) = (1 - \mu)^{1-\mu} \mu^\mu y_s(x, t) (r_s(x) + r_A)^{-\mu}. \quad (13)$$

3 Equilibrium

3.1 Equilibrium conditions

We assume that the commuters decide their residential locations in the long-run, whereas they choose their trip timings in the short-run, which is similar to the modeling of Gubins and Verhoef (2014), Takayama and Kuwahara (2017), and Takayama (2020). That is, the downtown commuters and suburban commuters at location x minimize commuting cost $C_d(t)$ and $C_s(x, t)$, respectively by selecting their arrival time t at work taking their residential locations as given in the short-run. Each commuter chooses a residential location (the downtown area or location x in the suburban area) so as to maximize his/her utility in the long-run.

3.1.1 Short-run equilibrium conditions

In the short-run, the commuters only decide their trip timing, which implies that the numbers of downtown commuters and suburban commuters residing at x are assumed to be fixed. The short-run equilibrium conditions differ according to their residential locations. According to Eq. (5a), all downtown commuters arrive at $t = t^*$, and they incur a constant commuting cost αT_d . Therefore, the short-run equilibrium cost C_d^* expressed as

$$C_d^* = \alpha T_d. \quad (14)$$

As for the suburban commuters, Eq. (5b) states that the commuting cost consists of the cost $\alpha\tau x$ of the suburban free-flow travel time, which depends only on the residential location x , and the bathtub cost $C_s^b(t)$ owing to the travel time in the downtown area and the schedule delay cost, which depends only on the arrival time t (i.e., $C_s^b(t) = \alpha T(t) + s(t)$). Thus, these commuters choose their arrival time such that the bathtub cost $C_s^b(t)$ is minimized. That is, no suburban commuter residing at x can reduce their bathtub cost by changing their departure time at the short-run equilibrium. The equilibrium conditions are

$$\begin{cases} C_s^b(t) = C_s^{b*} & \text{if } n(t) > 0 \\ C_s^b(t) \geq C_s^{b*} & \text{if } n(t) = 0 \end{cases} \quad \forall t \in \mathbb{R}, \quad (15a)$$

$$\int_{t \in \mathbb{R}} \frac{n(t)v(t)}{L} dt = N_s, \quad (15b)$$

where C_s^{b*} is the short-run equilibrium bathtub cost of the suburban commuters and N_s is the suburban population.

Condition (15a) states that if the bathtub cost at time t is greater than the equilibrium bathtub cost, then no one will arrive at their destination at time t . Condition (15b) is the conservation law for traffic demand in the suburban area. From these conditions, the congestion dynamics and the short-run equilibrium bathtub cost ($n(t)$ and C_s^{b*} , respectively) are endogenously determined at the short-run equilibrium. The short-run equilibrium cost $C_s^*(x)$ is expressed as expressed as

$$C_s^*(x) = C_s^{b*} + \alpha\tau x. \quad (16)$$

3.1.2 Long-run equilibrium conditions

Each commuter chooses a residential location (the downtown area or a location x in the suburban area) to maximize their indirect utility in the long run. Note that each commuter's residential location is determined based on the short-run equilibrium state (i.e., commuting cost). Therefore, as the short-run equilibrium cost C_d^* of the downtown commuters is given by Eq. (14), the income net of downtown commuting cost is

$$y_d = w - \alpha T_d. \quad (17)$$

Similarly, as the short-run equilibrium bathtub cost depends on the total number of suburban commuters, the income net of suburban commuting cost at x is expressed as

$$y_s(x) = w - C_s^{b*}(N_s) - \alpha \tau x. \quad (18)$$

The equilibrium conditions are

$$\begin{cases} U_d(y_d, r_d + r_A) = U^* & \text{if } N_d > 0 \\ U_d(y_d, r_d + r_A) \leq U^* & \text{if } N_d = 0 \end{cases}, \quad (19a)$$

$$\begin{cases} U_s(y_s(x), r_s(x) + r_A) = U^* & \text{if } N_s(x) > 0 \\ U_s(y_s(x), r_s(x) + r_A) \leq U^* & \text{if } N_s(x) = 0 \end{cases} \quad \forall x \in \mathbb{R}_+, \quad (19b)$$

$$\begin{cases} a_d(y_d, r_d + r_A)N_d = A_d & \text{if } r_d > 0 \\ a_d(y_d, r_d + r_A)N_d \leq A_d & \text{if } r_d = 0 \end{cases}, \quad (19c)$$

$$\begin{cases} a_s(y_s(x), r_s(x) + r_A)N_s(x) = A_s(x) & \text{if } r_s(x) > 0 \\ a_s(y_s(x), r_s(x) + r_A)N_s(x) \leq A_s(x) & \text{if } r_s(x) = 0 \end{cases} \quad \forall x \in \mathbb{R}_+, \quad (19d)$$

$$N_d + \int_{x \in \mathbb{R}_+} N_s(x) dx = N, \quad (19e)$$

where U^* is the long-run equilibrium utility level and $a_d(y_d, r_d + r_A)$ and $a_s(y_s(x), r_s(x) + r_A)$ denote the lot sizes of downtown commuters and suburban commuters who reside at location x , respectively. These lot sizes are given by

$$a_d(y_d, r_d + r_A) = \frac{\mu y_d}{r_d + r_A}, \quad (20a)$$

$$a_s(y_s(x), r_s(x) + r_A) = \frac{\mu y_s(x)}{r_s(x) + r_A}. \quad (20b)$$

Conditions (19a) and (19b) are the equilibrium conditions for the downtown and suburban residential location choices, respectively. These conditions state that no commuter has the incentive to change residential locations unilaterally. Conditions (19c) and (19d) are the land market clearing conditions, which states that if the total land demand for housing equals the land size, then land rent is (weakly) larger than the agricultural rent r_A . Condition (19e) shows the population constraint.

3.2 Equilibrium properties

3.2.1 Short-run equilibrium properties

As the short-run equilibrium condition (15) coincides with those in the bathtub model of Small and Chu (2003), we have the following properties.

Lemma 1. *The short-run equilibrium has the following properties*

- *The short-run equilibrium bathtub cost satisfies*

$$F(\theta) \equiv N_s - \alpha n_j \left(\frac{1}{\beta} + \frac{1}{\gamma} \right) \left(\ln \theta + \frac{1}{\theta} - 1 \right) = 0, \quad (21)$$

where $\theta \equiv \frac{C_s^{b*} v_f}{\alpha L}$.

- *Hypercongestion exists if $\theta > 2$.*

Proof. See Appendix A. □

As cases without hypercongestion are out of our interest, we impose the assumption that $\theta > 2$ from Lemma 1. All variables except the equilibrium bathtub cost C_s^{b*} are exogenous because the total number of suburban commuters N_s is given in the short-run. As the function of $F(\theta)$ is strictly monotone with respect to θ when $\theta > 2$, the equilibrium bathtub cost C_s^{b*} is uniquely determined.

The replacement of all human driven vehicles with autonomous vehicles influences the equilibrium bathtub cost. From Eq. (21), we obtain the following equation:

$$\frac{dC_s^{b*}}{dn_j} = - \left(\frac{\partial \theta}{\partial C_s^{b*}} \right)^{-1} \left(\frac{\partial F}{\partial \theta} \right)^{-1} \left(\frac{\partial F}{\partial n_j} \right) < 0. \quad (22)$$

As $\left(\frac{\partial \theta}{\partial C_s^{b*}} \right)^{-1}$ is positive and both of $\left(\frac{\partial F}{\partial \theta} \right)^{-1}$ and $\left(\frac{\partial F}{\partial n_j} \right)$ are negative, the network capacity effect (i.e., the increase in n_j) always decreases the equilibrium bathtub cost. This is because the network can process more vehicles due to the capacity expansion, so more commuters arrive at their destinations near their desired arrival times.

We also obtain the following equation from Eq. (21), which indicates that *the VOT effect (i.e., the reduction in α) may increase or decrease the equilibrium bathtub cost*:

$$\frac{dC_s^{b*}}{d\alpha} = - \left(\frac{\partial \theta}{\partial C_s^{b*}} \right)^{-1} \left(\frac{\partial F}{\partial \theta} \right)^{-1} \left(\frac{\partial F}{\partial \alpha} \right) \geq 0 \quad \text{if} \quad \frac{\partial F}{\partial \alpha} \leq 0, \quad (23)$$

$$\frac{\partial F}{\partial \alpha} = \frac{\partial f(\theta, \alpha)}{\partial \alpha} + \frac{\partial f(\theta, \alpha)}{\partial \theta} \frac{\partial \theta}{\partial \alpha}, \quad (24)$$

where $f(\theta, \alpha) = -\alpha n_j (\beta^{-1} + \gamma^{-1}) (\ln \theta + \theta^{-1} - 1)$ is the second term of $F(\theta)$. The first term on the RHS of Eq.(24) is negative and means that the VOT reduction simply decreases the bathtub congestion cost. The second term on the RHS of Eq.(24) is positive and means that a higher temporal concentration of traffic demand near the desired arrival time causes a more severe capacity drop and results in an increase in the bathtub congestion cost. Therefore, whether the equilibrium bathtub cost increases or decreases depends on the magnitudes of the network capacity and VOT effects.

Although the network capacity effect on hypercongestion has been extensively studied (e.g., Lu et al., 2020; Moshahedi and Kattan, 2022), the VOT effect on hypercongestion has been insufficiently explored. Most of the existing works investigating the network capacity effect consider autonomous vehicles to be beneficial (e.g., Fagnant and Kockelman, 2015; van den Berg and Verhoef, 2016; Lamotte et al., 2017). The only exception is van den Berg and Verhoef (2016), who examined both the effects of network capacity and VOT in the standard bottleneck model and showed that they *always* decrease the equilibrium travel cost. However, this may not hold in the presence of hypercongestion due to the capacity drop caused by the VOT effect. In other words, hypercongestion can worsen and the travel cost can increase when autonomous vehicles are introduced if the VOT effect is large.

The short-run equilibrium properties are summarized as follows.

Proposition 1. *The short-run equilibrium has the following properties.*

- *The short-run equilibrium bathtub cost is uniquely determined.*
- *The introduction of autonomous vehicles may increase or decrease the short-run equilibrium bathtub cost in the presence of hypercongestion.*

3.3 Long-run equilibrium properties

We examine the properties of the urban spatial structure at the long-run equilibrium.

Lemma 2. *At the long-run equilibrium,*

$$\frac{d\{r_s(x) + r_A\}}{dx} = -\alpha\tau \frac{r_s(x) + r_A}{\mu y_s(x)} < 0, \quad (25)$$

$$\frac{d\left\{\frac{N_s(x)}{A_s(x)}\right\}}{dx} = -\alpha\tau \frac{(1-\mu)(r_s(x) + r_A)}{\{\mu(w - C_s^{b*} - \alpha\tau x)\}^2} < 0. \quad (26)$$

Proof. See Appendix B. □

Lemma 2 indicates that the land rent and population density in the suburban area decrease with an increase in location x . These properties are consistent with those in the literature (e.g., Fujita, 1989). Then, the long-run equilibrium properties are as follows.

Lemma 3. *At the long-run equilibrium,*

- N_d^* and $N_s^*(x)$ are given by

$$N_d^* = \frac{1}{\mu} \{y_d\}^{\frac{1-\mu}{\mu}} (w - C_s^{b*})^{-\frac{1}{\mu}} (r_s(0) + r_A) A_d, \quad (27)$$

$$N_s^*(x) = \frac{1}{\mu} \{w - C_s^{b*} - \alpha\tau x\}^{\frac{1-\mu}{\mu}} \{y_d\}^{-\frac{1}{\mu}} (r_s(0) + r_A) A_s(x). \quad (28)$$

- *The city boundary x_f is given by*

$$x_f = \frac{w - C_s^{b*}}{\alpha\tau} (\{r_A\}^{-\mu} - \{r_s(0) + r_A\}^{-\mu}) \{r_A\}^{\mu}. \quad (29)$$

- $r_s(0)$ is determined from $\int_0^{x_f} N_s^*(x) dx = N - N_d^*$.

Proof. See Appendix C. □

Eq. (27) states that the downtown population decreases with a decrease in the short-run equilibrium bathtub cost. This occurs because a lower commuting cost encourages more commuters to choose the suburban area as their residential location. Combining Lemma 3 with Proposition 1 suggests that the introduction of autonomous vehicles does not necessarily result in an increase in the suburban population (i.e., suburbanization). That is, *the downtown population may increase due to the VOT effect, and thus the total car traffic demand decreases in the long-run.*

It should be noted that the VOT effect of autonomous vehicles decreases the cost of free-flow travel time in the suburban area, causing suburban commuters to reside farther from the downtown. This leads to a decrease in the population density in the suburban area and the spatial expansion of the city, as indicated by Eqs. (28) and (29). This is consistent with the standard results obtained in the literature. Therefore, *even if the introduction of autonomous vehicles leads to a decrease in the suburban population, the city can spatially expand outward.* In Section 6, we will demonstrate that such a case actually occurs.

The results are summarized as follows.

Proposition 2.

- *The introduction of autonomous vehicles (i.e., the VOT and network capacity effects) may increase the short-run equilibrium bathtub cost, resulting in a decrease in the suburban population (i.e., total car traffic demand) in the long-run.*
- *Even if the introduction of autonomous vehicles decreases the suburban population, the city may spatially expand outward.*

4 Perimeter Control

4.1 Perimeter control scheme

During perimeter control, the inflow rate to the downtown area is restricted to maintain the maximum throughput in the downtown area. A queue will develop outside the perimeter boundary if the arrival rate at the boundary exceeds the restricted inflow rate to the downtown area.

We derive the critical accumulation n_{cr} , where the throughput is maximized from Eq. (1).

$$n_{cr} = \frac{n_j}{2}. \quad (30)$$

The aim of perimeter control is to restrict the inflow at the perimeter boundary so as not to exceed the critical accumulation in the downtown area. Therefore, the inflow rate during perimeter control $I(t)$ is determined by

$$I(t) = \begin{cases} I_p & \text{if } n(t) = n_{cr} \\ A_b(t) & \text{if } n(t) < n_{cr} \end{cases}, \quad (31)$$

where I_p is the inflow rate during perimeter control and $A_b(t)$ is the arrival rate at the perimeter boundary at time t . If the accumulation is below the critical level, then no restriction is implemented; all vehicles at the boundary can enter the downtown area. Once accumulation reaches the critical accumulation, the inflow rate is restricted to I_p . The throughput can be maximized during perimeter control if the inflow rate $I(t)$ is set to the NEF at the critical accumulation. Thus, from Eqs. (1)-(3) and (30), we have

$$I_p = \frac{n_j v_f}{4L}. \quad (32)$$

4.2 Queuing dynamics at perimeter boundaries

A queue will develop outside the perimeter boundary if the arrival rate at the perimeter boundary exceeds the inflow rate I_p . We model the queuing dynamics as a point queue and assume a first-arrived-first-in property. Therefore, the waiting time of a commuter who arrives at their destination at time t , $T_w(t)$, is

$$T_w(t) = \frac{q(t)}{I_p}, \quad (33)$$

where $q(t)$ is the number of vehicles queued at the perimeter boundary when a commuter who arrives at their destination at time t reaches the boundary.

4.3 Schedule preferences of suburban commuters

The schedule preferences of the downtown commuters are the same as those without perimeter control in Eq. (5). Given the queue dynamics during perimeter control, suburban commuting cost $C_s^p(x, t)$ of a

commuter who resides at x and arrives at work at time t is

$$C_s^p(x, t) = \alpha(T^p(t) + \tau x) + s(t), \quad (34a)$$

$$T^p(t) = \begin{cases} T(t) & \text{if } t \leq t_s^p \\ \frac{L}{v_f/2} + T_w(t) & \text{if } t_s^p < t \leq t_e^p, \\ T(t) & \text{if } t_e^p < t \end{cases} \quad (34b)$$

$$s(t) = \begin{cases} \beta(t^* - t) & \text{if } t \leq t^* \\ \gamma(t - t^*) & \text{if } t > t^* \end{cases}, \quad (34c)$$

where $T^p(t)$ is the downtown travel time under perimeter control, which includes the travel time in the downtown area and the waiting time at the perimeter boundary. t_s^p and t_e^p are the start and end times of perimeter control, respectively. The difference between the schedule preferences at the equilibrium without and with perimeter control appears in the downtown travel time under perimeter control $T^p(t)$. The downtown travel time before and after perimeter control implementation ($t \leq t_s^p$ and $t_e^p < t$, respectively) are the same as Eq. (5). During perimeter control, the travel time in the downtown area is $\frac{L}{v_f/2}$ because the NEF is maintained at the maximum. Furthermore, waiting time at the perimeter boundary (Eq. (33)) is incurred in addition to the travel time in the downtown area.

5 Equilibrium under Perimeter Control

5.1 Equilibrium conditions

5.1.1 Short-run equilibrium

The short-run equilibrium conditions for the downtown commuters are the same as those without perimeter control (Section 3.1.1). Therefore,

$$C_d^{p*} = \alpha T_d, \quad (35)$$

where C_d^{p*} is the short-run equilibrium cost of the downtown commuters.

As at the short-run equilibrium without perimeter control, the suburban commuters choose their arrival times such that the bathtub cost ($C_s^{bp}(t) = \alpha T^p(t) + s(t)$) is minimized. Therefore, the equilibrium conditions are

$$\begin{cases} C_s^{bp}(t) = C_s^{bp*} & \text{if } n(t) > 0 \\ C_s^{bp}(t) \geq C_s^{bp*} & \text{if } n(t) = 0 \end{cases} \quad \forall t \in \mathbb{R}, \quad (36a)$$

$$\begin{cases} n(t) = \frac{n_j}{2} & \text{if } q(t) > 0 \\ n(t) \leq \frac{n_j}{2} & \text{if } q(t) = 0 \end{cases} \quad \forall t \in \mathbb{R}, \quad (36b)$$

$$\int_{t \in \mathbb{R}} \frac{n(t)v(t)}{L} dt = N_s, \quad (36c)$$

where C_s^{bp*} is the short-run equilibrium bathtub cost during perimeter control and N_s is the number of suburban commuters under perimeter control.

Conditions (36a) and (36c) are the same as Conditions (15a) and (15b), respectively. Condition (36b) reflects the restriction of the inflow to the downtown area during perimeter control; accumulation is at the critical level if there is a queue at the perimeter boundary. Otherwise, accumulation is lower than

the critical level. Then, the short-run equilibrium cost $C_s^{p*}(x)$ is

$$C_s^{p*}(x) = C_s^{bp*} + \alpha\tau x. \quad (37)$$

5.1.2 Long-run equilibrium

In the long-run, the difference between the cases with and without perimeter control appears only in the income net of suburban commuting cost. Specifically, under the perimeter control, the income net of suburban commuting cost at location x is

$$y_s^p(x) = w - C_s^{p*}(x). \quad (38)$$

The long-run equilibrium conditions are thus represented as (19) with the use of (38).

5.2 Equilibrium properties

5.2.1 Short-run equilibrium

Similar to the model of Dantsuji et al. (2023), we have the following properties.

Lemma 4. *The short-run equilibrium under perimeter control has the following properties*

- *The short-run equilibrium bathtub cost satisfies*

$$F^p(\theta^p) \equiv N_s - \alpha n_j \left(\frac{1}{\beta} + \frac{1}{\gamma} \right) \left(\frac{\theta^p}{4} + \ln 2 - 1 \right) = 0, \quad (39)$$

where $\theta^p \equiv \frac{C_s^{pb*} v_f}{\alpha L}$.

- *A queue develops at the perimeter boundary, and its length increases toward the desired arrival time.*

Proof. See Appendix D. □

All variables except the equilibrium bathtub cost C_s^{pb*} are exogenous. The equilibrium bathtub cost C_s^{pb*} is uniquely determined because the function of $F^p(\theta^p)$ is strictly monotone with respect to θ^p . Eq. (39) is rewritten as

$$C_s^{pb*} = \frac{\beta\gamma}{\beta + \gamma} \frac{N_s}{\frac{n_j v_f}{4L}} + \frac{4\alpha L}{v_f} (1 - \ln 2). \quad (40)$$

When autonomous vehicles are introduced, as shown in Eq. (40), *both the network capacity and VOT effects decrease the short-run equilibrium cost of the suburban commuters under perimeter control* (i.e., $dC_s^{pb*}/dn_j < 0$ and $dC_s^{pb*}/d\alpha > 0$, respectively). The network capacity effect increases the number of vehicles traveling in the downtown area during perimeter control and the restricted inflow rate at the perimeter boundary. Consequently, more suburban commuters arrive at their destinations near their desired arrival times. This decreases the short-run equilibrium cost of the suburban commuters.

Without perimeter control, the VOT effect may increase the short-run equilibrium cost for the suburban commuters due to capacity drop. With perimeter control, the VOT effect always decreases the short-run equilibrium cost because capacity drop never occurs. Even though the queue length at the perimeter boundary increases due to the VOT effect, the equilibrium cost decreases because the inflow rate is constant regardless of the queue length. This mechanism is the same as that in the standard bottleneck model (van den Berg and Verhoef, 2016) because this situation involves a bottleneck with a fixed capacity (i.e., the value of NEF at critical accumulation) between the downtown and suburban areas. Note that the first term on the RHS of Eq. (40) represents the bottleneck cost where the bottleneck

capacity is $\frac{n_j v_f}{4L}$, which is identical to the value of NEF at critical accumulation. This indicates that the impacts of autonomous vehicles in the presence of hypercongestion contradict those in the standard bottleneck model.

Next, we compare equilibria with and without perimeter control to demonstrate the effects of perimeter control on the urban spatial structure. The only difference between the cases with and without perimeter control appears in the short-run equilibrium bathtub cost (C_s^{b*} and C_s^{bpb*} , respectively). Eqs. (21) and (39) show that the short-run equilibrium bathtub cost is reduced by perimeter control when hypercongestion exists (see Appendix E for the proof). The short-run equilibrium bathtub cost decreases because network capacity drop never occurs under perimeter control. Thus, more commuters arrive at their destinations near their desired arrival times than at user equilibrium where capacity drop occurs. Therefore, *although queuing congestion occurs at the perimeter boundary, the short-run equilibrium bathtub cost decreases.*

The Properties of the short-run equilibrium with perimeter control are summarized as follows.

Proposition 3. *The short-run equilibrium with perimeter control has the following properties.*

- *The short-run equilibrium bathtub cost with perimeter control is uniquely determined.*
- *The introduction of autonomous vehicles decreases the short-run equilibrium bathtub cost under perimeter control.*
- *Hypercongestion mitigation by perimeter control decreases the short-run equilibrium bathtub cost.*

5.2.2 Long-run equilibrium

We investigate the properties of the urban spatial structure at the long-run equilibrium with perimeter control. In the long-run, the difference between cases with and without perimeter control is the income net of commuting cost. Thus, we have the following properties.

Lemma 5. *At the long-run equilibrium under perimeter control*

- N_d^{p*} and $N_s^{p*}(x)$ are given by

$$N_d^{p*} = \frac{1}{\mu} \{y_d\}^{\frac{1-\mu}{\mu}} (w - C_s^{bpb*})^{-\frac{1}{\mu}} (r_s(0) + r_A) A_d, \quad (41)$$

$$N_s^{p*}(x) = \frac{1}{\mu} \{w - C_s^{bpb*} - \alpha\tau x\}^{\frac{1-\mu}{\mu}} \{y_d\}^{-\frac{1}{\mu}} (r_s(0) + r_A) A_s(x). \quad (42)$$

- *The city boundary x_f is given by*

$$x_f = \frac{w - C_s^{bpb*}}{\alpha\tau} (\{r_A\}^{-\mu} - \{r_s(0) + r_A\}^{-\mu}) \{r_A\}^{\mu}. \quad (43)$$

- $r_s(0)$ is determined from $\int_0^{x_f} N_s^{p*}(x) dx = N - N_d^{p*}$.

Lemma 5 suggests that the urban spatial structure at the long-run equilibrium under perimeter control has the same properties as the cases without perimeter control. Specifically, Eq. (41) indicates that the downtown population decreases with a decrease in the short-run equilibrium bathtub cost. Eqs. (42) and (43) state that the VOT effect decreases the population density in the suburban area and expands the city outward. Therefore, as the introduction of autonomous vehicles always decreases the short-run equilibrium bathtub cost under perimeter control (Proposition 3), *the downtown population decreases under perimeter control due to the introduction of autonomous vehicles.*

As the short-run equilibrium bathtub cost is reduced by perimeter control (Proposition 3), the downtown population decreases in the long-run, which can be seen from Eq. (41). Since the income net of

Table 1: Numerical results of short-run equilibrium.

Case	C_s^{b*}	C_s^{bp*}	$\frac{C_s^{bp*}}{C_s^{b*}}$
Base case ($\eta = 1, \xi = 1$)	39.8	30.1	0.76
Case I ($\eta = 0.59, \xi = 1.029$)	54.8	26.9	0.49
Case II ($\eta = 0.76, \xi = 1.19$)	34.9	24.8	0.71

the suburban commuting cost increases, more commuters select the suburban area as their residential locations. Cities are expanded by hypercongestion mitigation.

The results are summarized as follows.

Proposition 4.

- *The introduction of autonomous vehicles under perimeter control decreases the short-run equilibrium bathtub cost, and results in a decrease in the downtown population in the long-run.*
- *Hypercongestion mitigation by perimeter control decreases the short-run equilibrium cost, and results in a decrease in the downtown population in the long-run.*

6 Numerical Examples

6.1 Short-run equilibrium

First, we numerically investigate the short-run equilibrium patterns to understand the short-run impacts of autonomous vehicles and perimeter control. We set the fixed suburban commuters to $N_s = 300$ [pax]. The other parameters related the short-run equilibrium are as follows: $v_f = 20$ [mph], $n_j = 100$ [veh], $\alpha, \beta, \gamma = 20, 10, 40$ [\$/h], $t^* = 0$, $L = 5$ [mile]. Based on the empirical studies on the impacts of autonomous vehicles (see the details in Section 2.1), we compare the equilibrium patterns of three cases: the case of base equilibrium (Base case); a case with the highest VOT and lowest network capacity effects of autonomous vehicles (Case I); and a case with the lowest VOT and highest network capacity effects of autonomous vehicles (Case II). In addition to the above parameters, we set the VOT effect parameter to $\eta = 0.59$ (Case I) and 0.76 (Case II), and the network capacity effect parameter to $\xi = 1.029$ (Case I) and 1.19 (Case II).

Figs. 2 - 6 show the equilibrium patterns for three cases. In all cases, a similar evolution of car accumulation is obtained as depicted in Fig. 2. The introduction of autonomous vehicles results in more vehicles circulating in the downtown area at the desired arrival time, due to the network capacity effect. The rush hour is longer in Case I and shorter in Case II than that in the Base case. This indicates that the introduction of autonomous vehicles increases and decreases the short-run equilibrium bathtub cost in Case I and II, respectively, as shown in Table 1.

Fig. 3 reveals that the speed at the desired arrival time in Case II is higher than that in Case I, although the maximum accumulation observed at the desired arrival time in Case II is higher than that in Case I due to the higher network capacity effect in Case II. This leads to the higher NEF in Case II when the maximum accumulation is reached, as depicted in Fig. 4. Moreover, even though the maximum accumulation in Case II is higher than that in the Base case in the hypercongested regime, the NEF in Case II is higher than that in the Base case (with human-driven vehicles) at their maximum accumulation. Therefore, a lighter capacity drop is observed in Case II, as depicted in Fig. 5, leading to a shorter rush hour and resulting in a decrease in the short-run equilibrium bathtub cost.

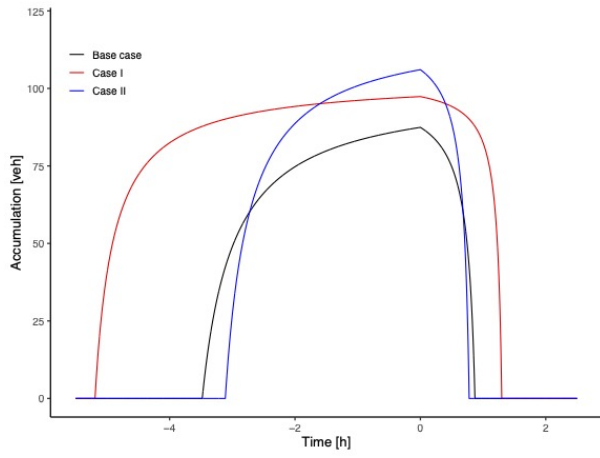


Figure 2: Accumulation in the downtown area

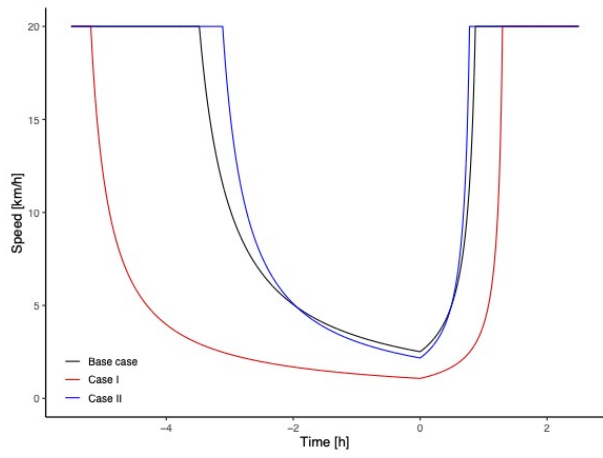


Figure 3: Speed in the downtown area

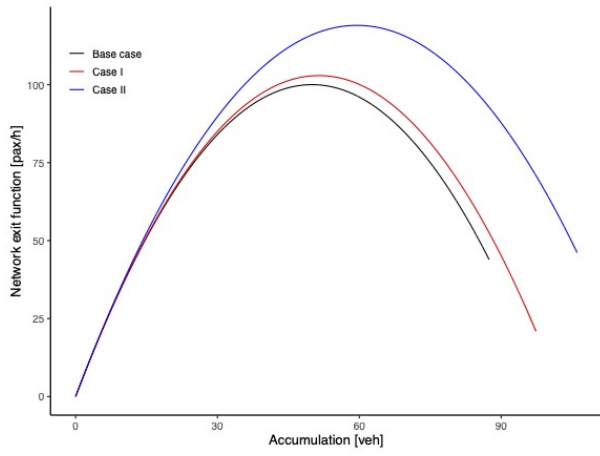


Figure 4: MFD in the downtown area.

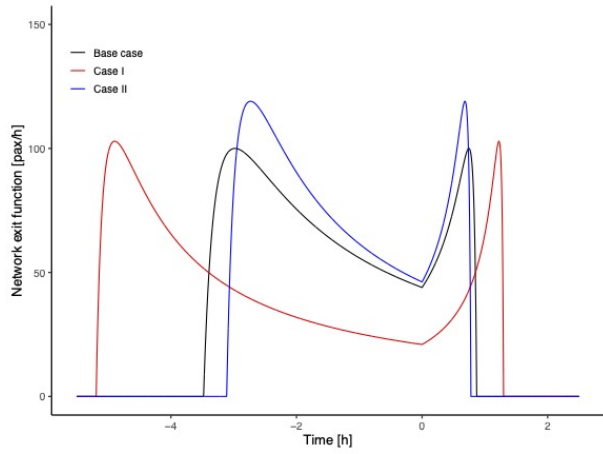


Figure 5: NEF of suburban commuters in downtown area

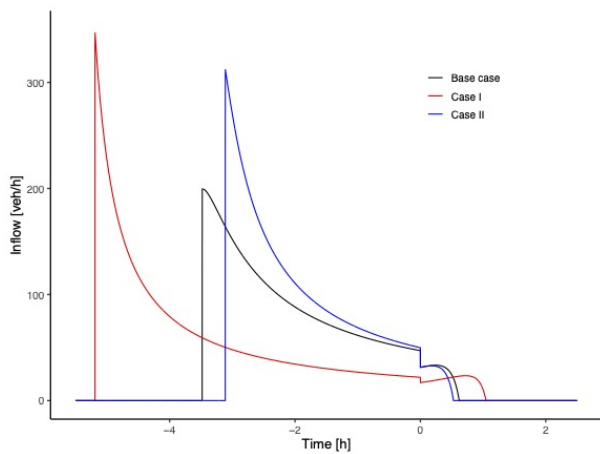


Figure 6: Inflow in downtown area

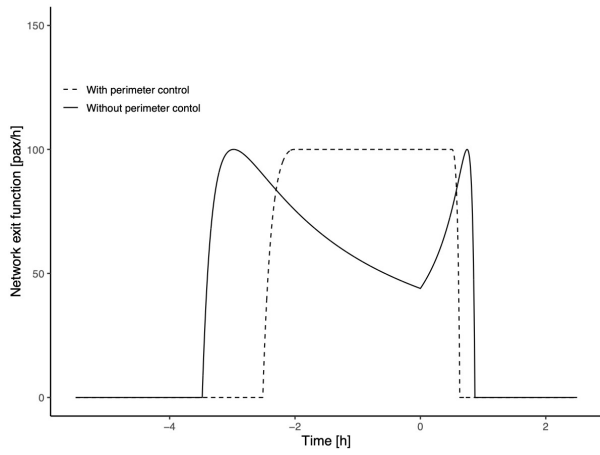


Figure 7: NEF with and without perimeter control (base case)

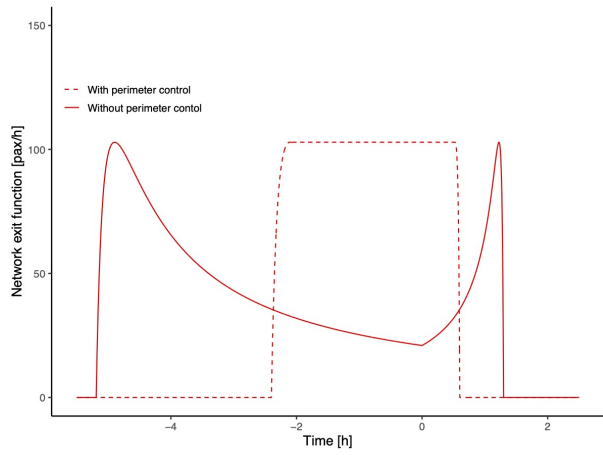


Figure 8: NEF with and without perimeter control (Case I)

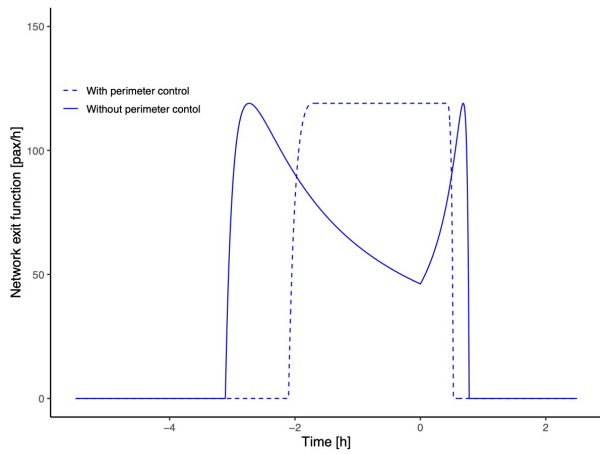


Figure 9: NEF with and without perimeter control (Case II)

Table 2: Numerical results of short-run and long-run equilibria.

Case	N_s	C_s^{b*}	U^*	N_s^p	C_s^{bp*}	U^{p*}
Base case ($\eta = 1, \xi = 1$)	224.0	27.8	4.594	252.2	26.3	4.684
I ($\eta = 0.59, \xi = 1.029$)	221.2	31.4	4.586	305.5	27.4	4.883
II ($\eta = 0.76, \xi = 1.19$)	256.6	28.1	4.699	308.1	25.4	4.894

superscript p describes variables under perimeter control.

Conversely, the higher temporal concentration of traffic demand (Fig. 6), due to the high VOT effect, induces a more severe capacity drop in Case I compared to the Base case and Case II. This results in an increase in the short-run equilibrium bathtub cost. Therefore, the introduction of autonomous vehicles may increase or decrease the short-run equilibrium bathtub cost in the presence of hypercongestion.

Perimeter control implementation shortens the rush hour and results in a decrease in the short-run equilibrium bathtub cost in all cases, as illustrated in Figs. 7 - 9. Since hypercongestion never occurs under perimeter control, more commuters arrive at their destinations near their desired arrival times, which results in a shorter rush hour. Note that the applied perimeter control strategy is similar to that proposed in Daganzo (2007). Even if other advanced control strategies, such as reinforcement learning-based approach (Chen et al., 2022a), aiming at maximizing throughput in the downtown area are employed, the short-run bathtub equilibrium cost would remain the same. This results in the same impact on the long-run equilibrium as the perimeter control strategy applied in this paper. It is also important to note that the control inflow could be influenced by various factors such as the network infrastructure (e.g., Aboudolas and Geroliminis, 2013), it can be challenging to set the targeted accumulation precisely at the critical value. Such biases are investigated in Appendix F.

To further investigate the effect of perimeter control, we estimate the ratio of the short-run bathtub equilibrium cost with perimeter control to that without perimeter control as shown in the last column of Table 1. Given that the duration of hypercongestion is longest and a severe capacity drop occurs in Case I among the three cases, the effect of perimeter control is the largest in Case I. Although the duration of hypercongestion is shorter in Case II compared to the Base case, the effect of perimeter control is larger in Case II due to more temporal concentration of traffic demand (Fig. 6) and higher network capacity.

6.2 Short-run and long-run equilibria

We next investigate the equilibrium patterns including the long-run equilibrium. Instead of using the fixed constant suburban commuters in Section 6.1, the total population is set to $N = 600$ [pax]. We also set the parameters related to the long-run equilibrium as follows: $r_A = 30$, $w = 60$, $\mu = 0.25$, $A_d = 2$, and $A_s(x) = 1$. We use the same cases as in Section 6.1 to compare the impact of autonomous vehicles and hypercongestion mitigation by perimeter control on the equilibrium patterns.

Table. 2 shows that the introduction of autonomous vehicles decreases and increases the suburban population in Case I and II, respectively. When autonomous vehicles are introduced, less commuters choose the suburban area as the residential location in the long-run due to an increases in the short-run equilibrium bathtub cost in Case I and more commuters choose the suburban area in the long-run due to a decrease in the short-run equilibrium bathtub cost in Case II. Even though the suburban population in Case I is lower than that in the base case, the short-run equilibrium bathtub cost increases (i.e., longer rush hour in Figs. 10 and 11) due to a severe capacity drop (Figs. 12 and 13) by more temporal concentration of traffic demand by the VOT effect (Fig. 14). On the other hand, the higher suburban

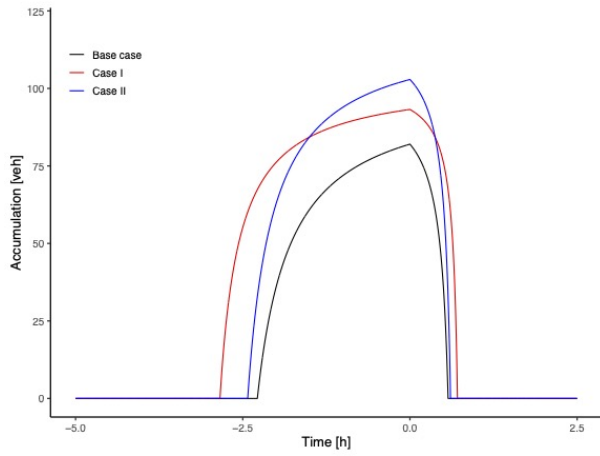


Figure 10: Accumulation in the downtown area

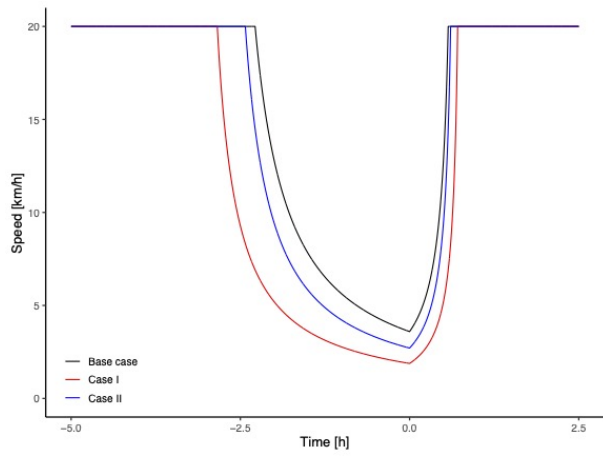


Figure 11: Speed in the downtown area

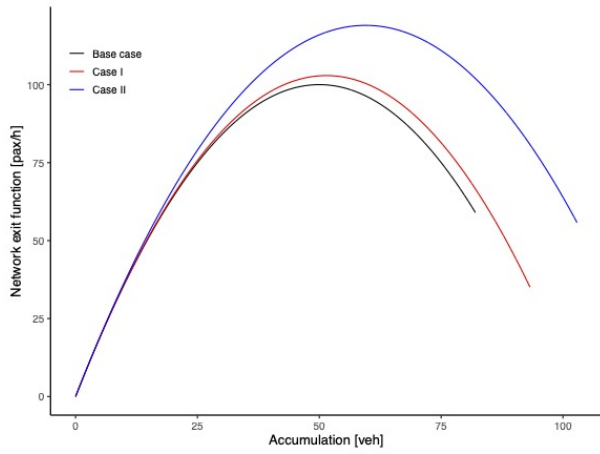


Figure 12: MFD in the downtown area.

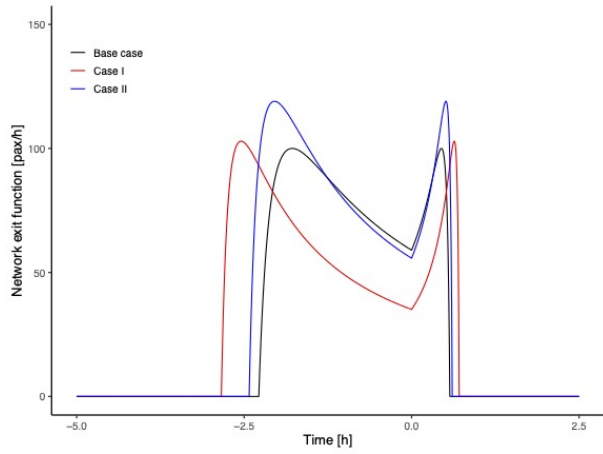


Figure 13: NEF of suburban commuters in downtown area

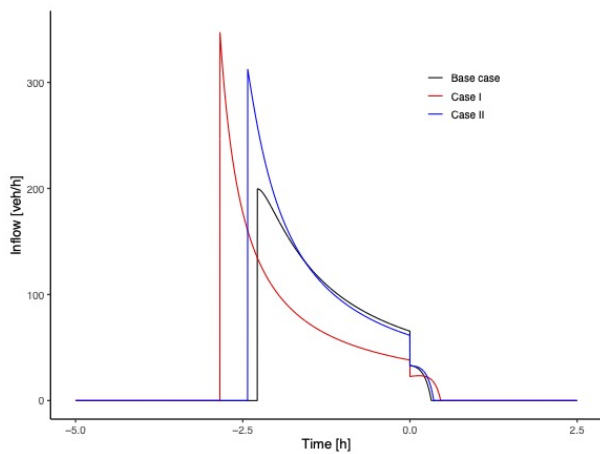


Figure 14: Inflow in downtown area

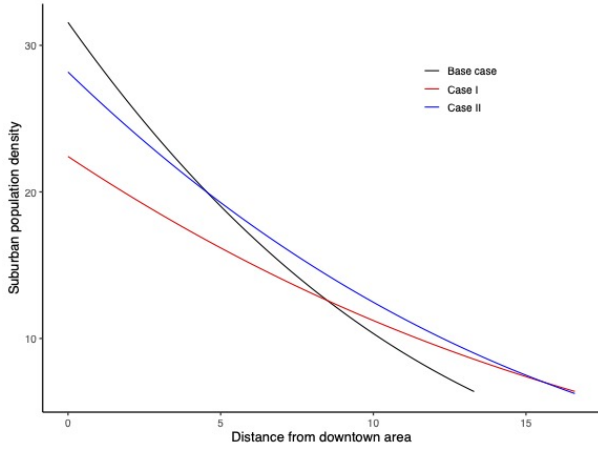


Figure 15: Suburban population density by residential location

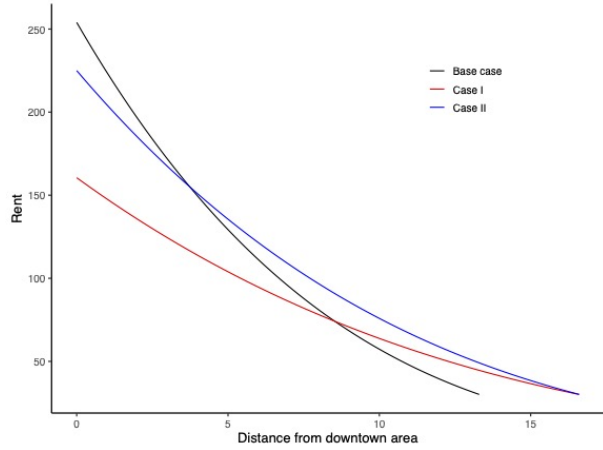


Figure 16: Rent by residential location

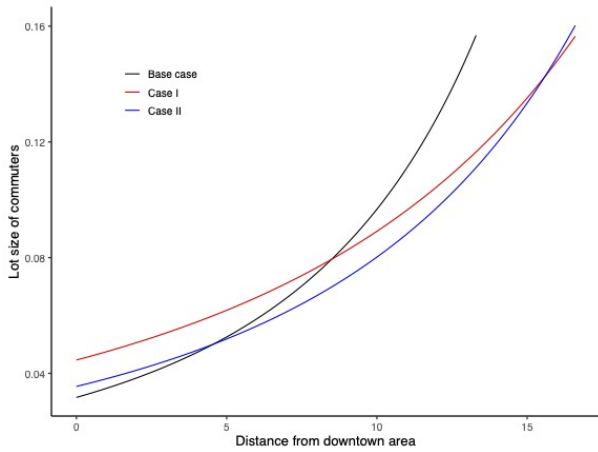


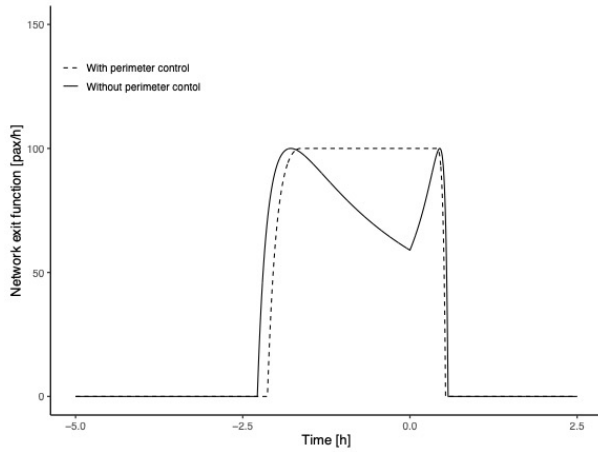
Figure 17: Lot size of commuters by residential location

population leads to an increase in the short-run equilibrium bathtub cost in Case II.

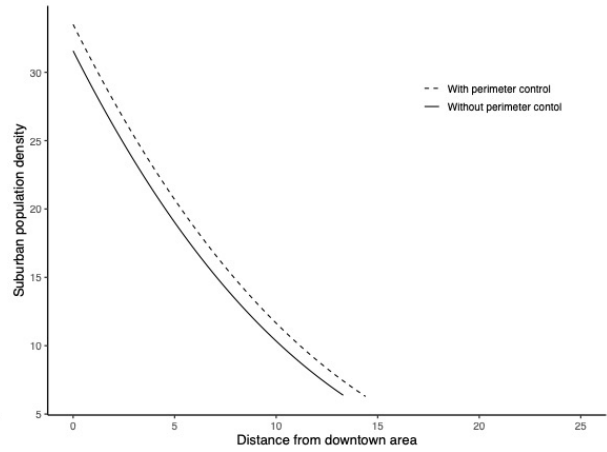
Although the suburban population decreases in Case I by the introduction of autonomous vehicles, the city spatially expand outward, as depicted in Figs. 15 - 17. This is because as the VOT effect is higher, suburban commuters care less about free-flow travel time in the suburban areas, which results in the farther city boundary. Interestingly, Table 2 reveals that the utility level may decrease despite that commuters can relocate in response to the changes in their commuting behaviors due to the introduction of autonomous vehicles. Therefore, the introduction of autonomous vehicles may decrease the utility level in the long-run due to a severe capacity drop in the short-run.

As perimeter control implementation decreases the short-run equilibrium bathtub cost, the suburban population increases, which results in the city expansion, as depicted in Table 2 and Figs. 18 - 20. Thus, hypercongestion mitigation by perimeter control decreases the short-run equilibrium bathtub cost, and results in a decrease in the downtown population in the long-run.

The short-run equilibrium bathtub cost in Case I is higher than that in the Base case with and without perimeter control, but the utility level is lower without perimeter control and higher with perimeter control in Case I than those in the Base case. This is because unlike the case in the presence of hypercongestion, the short-run equilibrium bathtub cost decreases with perimeter control and more commuters reside in

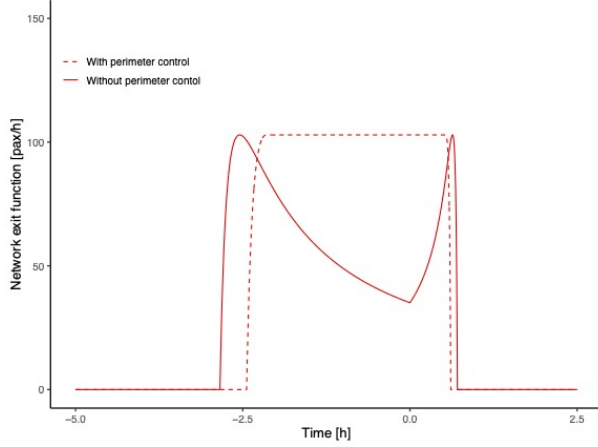


(a) NEF

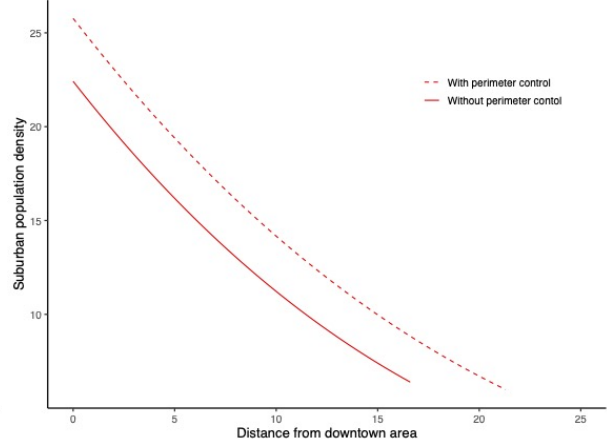


(b) Suburban population density

Figure 18: Base case

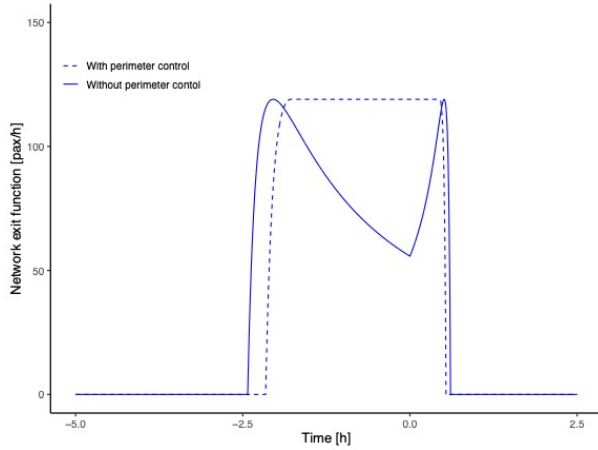


(a) NEF

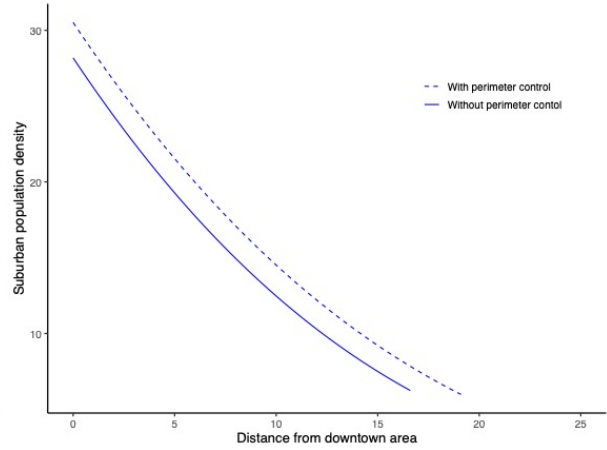


(b) Suburban population density

Figure 19: Case I



(a) NEF



(b) Suburban population density

Figure 20: Case II

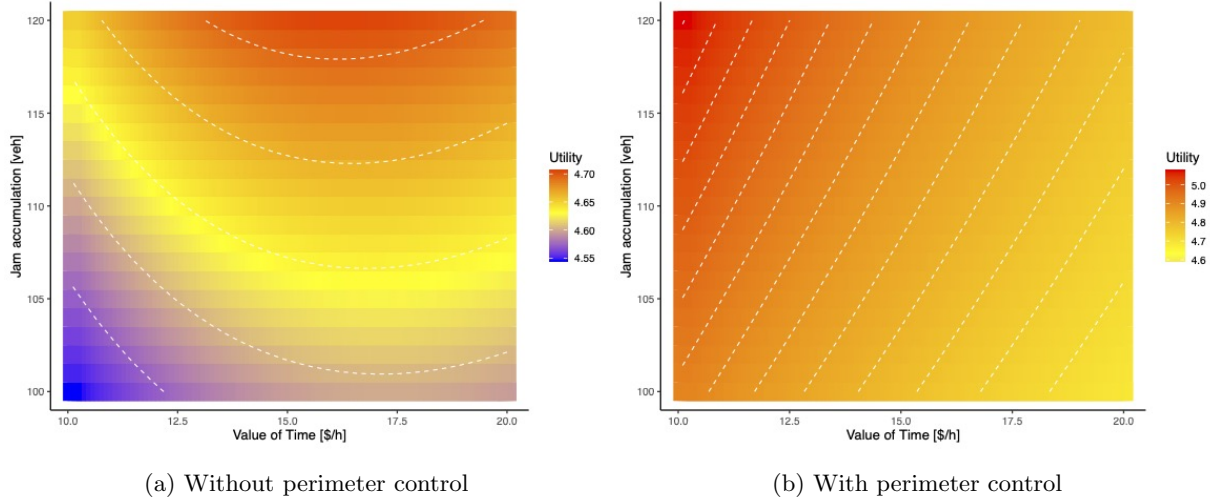


Figure 21: Sensitivity analysis of utility

the suburban area in the long-run. Furthermore, the high VOT effect decreases the suburban population density at location x . Thus, both the short-run equilibrium bathtub cost and the utility level are higher in Case I than in the Base case. The same effects exist in Case II. However, the high network capacity effect causes more suburban commuters to arrive at their destinations in the short-run, but the low VOT effect causes a higher suburban population density and results in fewer commuters residing in the suburban area in the long-run compared with Case I. Thus, the short-run equilibrium bathtub cost is lower, but the utility level is higher in Case II than in the Base case.

Next, we conduct a sensitivity analysis of utility with respect to both the network capacity and VOT effects, as depicted in Fig. 21. The pictures of the utility levels with and without perimeter control change entirely. Without perimeter control, both the network capacity and the VOT effects increase the utility level when the VOT effect is low (i.e., high value of time in Fig. 21a). However, the utility level begins to decrease when the VOT effect exceeds the threshold values. This is because a high VOT effect leads to a severe capacity drop, resulting in an increase in the short-run equilibrium bathtub cost. Consequently, the income net of the suburban commuting cost decreases and the downtown population increases, leading to a lower utility level in the long-run. When the VOT effect is low, the short-run equilibrium bathtub cost decreases, and the free-flow travel time cost in the suburban area also decreases, resulting in a higher utility level. When perimeter control is implemented, both network capacity and VOT effects always increase the utility level, as depicted in Fig. 21b. As discussed earlier, both effects consistently decrease the short-run equilibrium bathtub cost, resulting in an increase in income net of the suburban commuting cost and a decrease in the downtown population. They contribute to a higher utility level.

7 Conclusions

In this paper, by incorporating a bathtub model, we develop a land use model where hypercongestion occurs in the downtown area and interacts with land use to examine the effects of hypercongestion mitigation by perimeter control and the introduction of autonomous vehicles on the spatial structures of cities. The results indicate that (I) hypercongestion mitigation decreases the commuting cost and results in a less dense urban spatial structure, (II) the introduction of autonomous vehicles may increase the commuting cost in the presence of hypercongestion and results in a decrease in the suburban population (i.e., total car traffic demand) in the long-run, but make cities spatially expanded outward, and (III) the

introduction of autonomous vehicles under perimeter control decreases the commuting cost and results in a less dense urban spatial structure. We also show that the introduction of autonomous vehicles may decrease the utility level in the long-run due to a severe capacity drop in the short-run. These results show that hypercongestion is a key factor that can change urban spatial structure. Specifically, the effect of autonomous vehicles on the urban spatial structures depends on the presence of hypercongestion. Moreover, the effect of autonomous vehicles on the urban spatial structure in the presence of hypercongestion contradicts that in the standard bottleneck model.

This paper has several future directions. First, we assumed commuter homogeneity. Incorporating heterogeneity such as in trip length (e.g., Fosgerau, 2015; Lamotte and Geroliminis, 2018) and preferences (e.g., Hall, 2018; Takayama and Kuwahara, 2020) is an interesting direction. Particularly, since changes in the OD demand patterns in the downtown area can impact the shape of the MFD, incorporating the city structure of the downtown area and the trip-based bathtub model is worth investigating. Second, we assumed a unimodal transportation system. Future models can be extended to multimodal transportation systems (e.g., Dantsuji et al., 2023). Third, we examined a scenario where all human-driven vehicles are replaced by autonomous vehicles. Extending it to scenarios involving mixed traffic of autonomous and human-driven vehicles would be desirable. Although there are some studies on the mixed traffic of autonomous and human-driven vehicles in the standard bottleneck model with heterogeneous commuters (e.g., van den Berg and Verhoef, 2016; Wu and Li, 2023), developing a mixed bimodal bathtub model with heterogeneous commuters in terms of value of travel time remains a challenging task, which represents one of the important future directions. Finally, the monocentric city structure in this work can be extended to a polycentric city structure and/or multi-region traffic systems.

Acknowledgements

We thank Se-il Mun, Tatsuhiko Kono, Minoru Osawa, and Koki Satsukawa for their valuable comments. This work was supported by JST ACT-X, Japan (grant #JPMJAX21AE), by JST FOREST Program, Japan (grant #JPMJFR215M), by JSPS KAKENHI, Japan (grant #23K13422 and #22H01610).

Appendix A: proof of Lemma 1

As Small and Chu (2003) assumed the Ardekani–Herman formula (i.e., $v(t) = v_f (1 - n(t)/n_j)^{1+\rho}$, where ρ is a parameter) for the space-mean speed in the downtown area, the Greenshields model in this paper can be regarded as a special case of the Small and Chu (2003) model where $\rho = 0$. Here, we briefly review the solution of the bathtub model. Differentiating the bathtub cost $C_s^b(t) = \alpha T(t) + s(t)$ with respect to time at equilibrium (i.e., $dC_s^b(t)/dt = 0$) yields

$$\frac{dT(t)}{dt} = \begin{cases} \frac{\beta}{\alpha} & \text{if } t \leq t^* \\ -\frac{\gamma}{\alpha} & \text{if } t > t^*. \end{cases} \quad (44)$$

From Eqs. (1) and (4), we have

$$\frac{dT(t)}{dt} = \frac{L}{n_j v_f} \left(1 - \frac{n(t)}{n_j}\right)^{-2}. \quad (45)$$

Combining Eqs. (44) and (45), grouping the terms in $n(t)$ and the other terms on the LHS and RHS, respectively, and integrating both sides yields

$$n(t) = \begin{cases} n_j \left(1 - \frac{1}{\frac{\beta v_f}{\alpha L} t + C_e} \right) & \text{if } t \leq t^* \\ n_j \left(1 - \frac{1}{-\frac{\gamma v_f}{\alpha L} t + C_l} \right) & \text{if } t > t^*, \end{cases} \quad (46)$$

where C_e and C_l are constants of integration for earliness and lateness, respectively. Since the accumulation at the start and end of the rush hour is zero (i.e., $n(t_s) = n(t_e) = 0$),

$$n(t) = \begin{cases} n_j \left(1 - \frac{1}{1 + \frac{\beta v_f}{\alpha L} (t - t_s)} \right) & \text{if } t \leq t^* \\ n_j \left(1 - \frac{1}{1 + \frac{\gamma v_f}{\alpha L} (t_e - t)} \right) & \text{if } t > t^*, \end{cases} \quad (47)$$

From Condition (15b),

$$N_s = \alpha n_j \left(\frac{1}{\beta} + \frac{1}{\gamma} \right) \left(\log \theta + \frac{1}{\theta} - 1 \right), \quad (48)$$

where $\theta = \frac{C_s^{b^*} v_f}{\alpha L}$.

When $\theta = 2$, the maximum accumulation reached during the rush hour is the critical accumulation ($n_j/2$) at the desired arrival time ($n(t^*) = n_j/2$). Therefore, hypercongestion exists if $\theta > 2$.

Appendix B: proof of Lemma 2

As $\frac{dU_s(x)}{dx} = 0$ at long-run equilibrium, we have from Eq. (25),

$$\frac{dr_s(x) + r_A}{dx} = -\alpha\tau \frac{r_s(x) + r_A}{\mu y_s(x)}. \quad (49)$$

The RHS is negative.

Combining Condition (19d) and Eq. (20a) yields

$$\frac{N_s(x)}{A_s(x)} = \frac{r_s(x) + r_A}{\mu y_s(x)}. \quad (50)$$

By differentiating Eq. (50) with respect to x and substituting Eq. (49) into Eq. (50), we obtain

$$\frac{d\frac{N_s(x)}{A_s(x)}}{dx} = -\alpha\tau \frac{(1 - \mu)(r_s(x) + r_A)}{\{\mu(w - C_s^{b^*} - \alpha\tau x)\}^2}. \quad (51)$$

The RHS is negative.

Appendix C: proof of Lemma 3

At the long-run equilibrium, the indirect utility satisfies $U_d^* = U_s^*(x)$ for all $x \in [0, x_f]$, and this condition gives

$$\frac{r_d + r_A}{r_s(x) + r_A} = \left(\frac{y_d}{y_s(x)} \right)^{\frac{1}{\mu}}. \quad (52)$$

As we have $a_d = \frac{A_d}{N_d}$ from Condition (19c), substituting these into Eq. (20a) results in N_d^* as follows.

$$N_d^* = \frac{1}{\mu} \{y_d\}^{\frac{1-\mu}{\mu}} (w - C_s^{b^*})^{-\frac{1}{\mu}} (r_s(0) + r_A) A_d. \quad (53)$$

Similarly, we have

$$N_s(x) = \frac{1}{\mu} \{w - C_s^{b*} - \alpha\tau x\}^{\frac{1-\mu}{\mu}} \{y_d\}^{-\frac{1}{\mu}} (r_s(0) + r_A) A_s(x). \quad (54)$$

Furthermore, as $U_s^*(0) = U_s^*(x_f)$, we obtain

$$x_f = \frac{w - C_s^{b*}}{\alpha\tau} (\{r_A\}^{-\mu} - \{r_s(0) + r_A\}^{-\mu}) \{r_A\}^\mu. \quad (55)$$

Appendix D: proof of Lemma 4

As the NEF is maintained at the maximum during perimeter control, the number of suburban commuters who arrive at their destinations during perimeter control is

$$N_s^p = \frac{n_j v_f}{4L} (t_e^p - t_s^p). \quad (56)$$

Since $C_s^{p*} = 2\alpha L/v_f + \beta(t^* - t_s^p) = 2\alpha L/v_f + \beta(t_e^p - t^*)$, substituting it into Eq. (56) produces

$$N_s^p = \frac{\alpha n_j}{4} \left(\frac{1}{\beta} + \frac{1}{\gamma} \right) (\theta^p - 2). \quad (57)$$

According to Eq. (47), the start and end times of perimeter control (t_s^p and t_e^p , respectively; $n(t_s^p) = n(t_e^p) = n_j/2$) are

$$t_s^p - t_s = \frac{1}{\beta} \frac{\alpha L}{v_f}, \quad (58)$$

$$t_e - t_e^p = \frac{1}{\gamma} \frac{\alpha L}{v_f}. \quad (59)$$

Therefore, the number of suburban commuters who arrive at their destinations before and after perimeter control is computed using Eqs. (1), (47), (58), and (59) as follows:

$$\begin{aligned} N_s^{op} &= \int_{t_s}^{t_s^p} \frac{n(s)v(s)}{L} ds + \int_{t_e^p}^{t_e} \frac{n(s)v(s)}{L} ds \\ &= \alpha n_j \left(\frac{1}{\beta} + \frac{1}{\gamma} \right) \left(\ln 2 - \frac{1}{2} \right). \end{aligned} \quad (60)$$

We combine Eqs. (57) and (60), and the number of suburban commuters is expressed as

$$N_s = \alpha n_j \left(\frac{1}{\beta} + \frac{1}{\gamma} \right) \left(\frac{\theta^p}{4} + \ln 2 - 1 \right). \quad (61)$$

Next, we prove that a queue develops at the perimeter boundary, and its length increases toward the desired arrival time. Eq. (34) and Condition (36a) yield

$$\begin{cases} \alpha \frac{dT_w(t)}{dt} - \beta = 0 \\ \alpha \frac{dT_w(t)}{dt} + \gamma = 0. \end{cases} \quad (62)$$

Combining this with Eq. (33), where I_p is constant, we obtain

$$\begin{cases} \frac{dq(t)}{dt} = \frac{\beta}{\alpha} \\ \frac{dq(t)}{dt} = -\frac{\gamma}{\alpha}. \end{cases} \quad (63)$$

Thus, a queue starts to develop once perimeter control is implemented, and its length increases toward the desired arrival time. Then its length decreases after the desired arrival time.

Appendix E: proof of $C_s^{b*} > C_s^{pb*}$

When hypercongestion exists without perimeter control, $\theta > 2$ from Lemma 1. Consider a set of parameters (including N_s), Ψ , where there exists $\theta(> 2)$ such that $F(\theta) = 0$. Under Ψ , it always holds that $F^p(\theta) < 0$. This leads to $\theta > \theta^p$ under Ψ if there exists $\theta^p(> 2)$ such that $F^p(\theta^p) = 0$. $\theta > \theta^p$ yields $C_s^{b*} > C_s^{pb*}$, which completes the proof.

Appendix F: biases in the critical accumulation estimation

Since the controlled inflow could be influenced by various factors such as infrastructure limitation (Aboudolas and Geroliminis, 2013), the selection of measurement points for the MFD estimation (Ortigosa et al., 2015), and the estimation methods (Leclercq et al., 2014), it is important to investigate the effects of these biases. To this end, we introduce the bias factor into the critical accumulation.

$$n_{cr} = \frac{\epsilon n_j}{2}, \quad (64)$$

where $\epsilon (> 0)$ is the bias factor caused by the reasons mentioned above. $\epsilon > 1$ indicates the accumulation under perimeter control is above the critical value.

As the only difference from the non-biased perimeter control is the bias factor ϵ , in the same way as Section 4, we have the short-run equilibrium bathtub cost satisfying

$$\begin{aligned} F_\epsilon^p(\theta_\epsilon^p) &\equiv \\ N_s - \alpha n_j \left(\frac{1}{\beta} + \frac{1}{\gamma} \right) &\left(\frac{\epsilon(2-\epsilon)}{4} \theta_\epsilon^p + \ln \frac{2}{2-\epsilon} - \epsilon \right) \\ &= 0. \end{aligned} \quad (65)$$

Note that if the critical accumulation estimation is not biased (i.e., $\epsilon = 1$), Eq. (65) is identical to Eq. (39).

We then conduct the numerical analyses for two cases: (A) higher accumulation than the critical value ($\epsilon = 1.3$), and (B) lower accumulation than the critical value ($\epsilon = 0.7$). Note that the outflow under perimeter control is maintained at the same level for both cases, but the traffic state is hypercongested in Case (A) and congested in Case (B). Fig. 22 displays the NEFs for the cases including the non-biased case ($\epsilon = 1$) and the case without perimeter control (UE).

We observe that the rush hour of the non-biased case is the shortest because the outflow can be maintained at its maximum, leading to the lowest short-run bathtub equilibrium cost. Interestingly, the rush hour in Case (A) is shorter than that in Case (B), even though the accumulation under perimeter control is in a hypercongested state for Case (A). This is because the maximum outflow is never reached for Case (B), while there are time windows in Case (A) when the outflow is higher than the outflow under perimeter control.

Since the traffic dynamics is unstable in the hypercongested state, further investigation is required. However, the obtained result suggests the possibility that controlling the inflow such that the outflow is slightly below the optimal value may be less effective than controlling the inflow such that the outflow is slightly above the optimal value.

References

Aboudolas, K. and Geroliminis, N. (2013). Perimeter and boundary flow control in multi-reservoir heterogeneous networks. *Transportation Research Part B: Methodological*, 55:265–281.

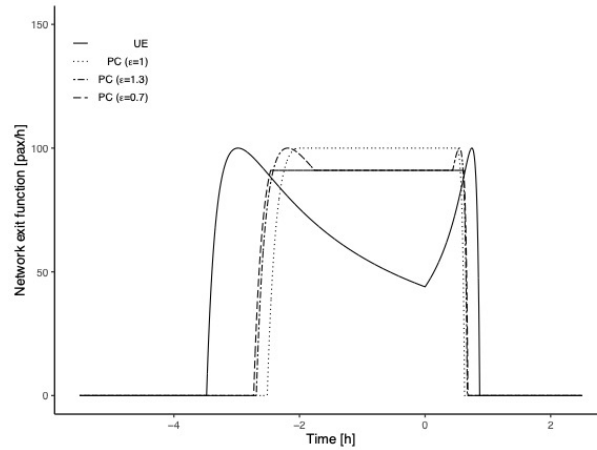


Figure 22: Impact of bias in the critical accumulation estimation

- Alonso, W. (1964). Location and land use. *Harvard university press*.
- Ameli, M., Faradonbeh, M. S. S., Lebacque, J.-P., Abouee-Mehrizi, H., and Leclercq, L. (2022). Departure time choice models in urban transportation systems based on mean field games. *Transportation Science*, 56(6):1483–1504.
- Ampountolas, K., Zheng, N., and Geroliminis, N. (2017). Macroscopic modelling and robust control of bi-modal multi-region urban road networks. *Transportation Research Part B: Methodological*, 104:616–637.
- Anas, A., Arnott, R., and Small, K. A. (1998). Urban spatial structure. *Journal of economic literature*, 36(3):1426–1464.
- Arnott, R. (1998). Congestion tolling and urban spatial structure. *Journal of regional science*, 38(3):495–504.
- Arnott, R. (2013). A bathtub model of downtown traffic congestion. *Journal of Urban Economics*, 76:110–121.
- Arnott, R., de Palma, A., and Lindsey, R. (1993). A structural model of peak-period congestion: A traffic bottleneck with elastic demand. *The American Economic Review*, pages 161–179.
- Bao, Y., Verhoef, E. T., and Koster, P. (2021). Leaving the tub: The nature and dynamics of hyper-congestion in a bathtub model with a restricted downstream exit. *Transportation Research Part E: Logistics and Transportation Review*, 152:102389.
- Batista, S. F., Ingole, D., Leclercq, L., and Menéndez, M. (2021). The role of trip lengths calibration in model-based perimeter control strategies. *IEEE Transactions on Intelligent Transportation Systems*, 23(6):5176–5186.
- Chen, C., Huang, Y., Lam, W., Pan, T., Hsu, S., Sumalee, A., and Zhong, R. (2022a). Data efficient reinforcement learning and adaptive optimal perimeter control of network traffic dynamics. *Transportation Research Part C: Emerging Technologies*, 142:103759.
- Chen, S., Fu, H., Wu, N., Wang, Y., and Qiao, Y. (2022b). Passenger-oriented traffic management integrating perimeter control and regional bus service frequency setting using 3d-pmfd. *Transportation Research Part C: Emerging Technologies*, 135:103529.

- Chiabaut, N. (2015). Evaluation of a multimodal urban arterial: The passenger macroscopic fundamental diagram. *Transportation Research Part B: Methodological*, 81:410–420.
- Daganzo, C. F. (2007). Urban gridlock: Macroscopic modeling and mitigation approaches. *Transportation Research Part B: Methodological*, 41(1):49–62.
- Dantsuji, T., Fukuda, D., and Zheng, N. (2021). Simulation-based joint optimization framework for congestion mitigation in multimodal urban network: a macroscopic approach. *Transportation*, 48(2):673–697.
- Dantsuji, T., Hirabayashi, S., Ge, Q., and Fukuda, D. (2020). Cross comparison of spatial partitioning methods for an urban transportation network. *International Journal of Intelligent Transportation Systems Research*, 18:412–421.
- Dantsuji, T., Hoang, N. H., Zheng, N., and Vu, H. L. (2022). A novel metamodel-based framework for large-scale dynamic origin–destination demand calibration. *Transportation Research Part C: Emerging Technologies*, 136:103545.
- Dantsuji, T., Takayama, Y., and Fukuda, D. (2023). Perimeter control in a mixed bimodal bathtub model. *Transportation Research Part B: Methodological*, 173:267–291.
- de Almeida Correia, G. H., Loeff, E., van Cranenburgh, S., Snelder, M., and van Arem, B. (2019). On the impact of vehicle automation on the value of travel time while performing work and leisure activities in a car: Theoretical insights and results from a stated preference survey. *Transportation Research Part A: Policy and Practice*, 119:359–382.
- Ding, H., Guo, F., Zheng, X., and Zhang, W. (2017). Traffic guidance–perimeter control coupled method for the congestion in a macro network. *Transportation Research Part C: Emerging Technologies*, 81:300–316.
- Fagnant, D. J. and Kockelman, K. (2015). Preparing a nation for autonomous vehicles: opportunities, barriers and policy recommendations. *Transportation Research Part A: Policy and Practice*, 77:167–181.
- Fosgerau, M. (2015). Congestion in the bathtub. *Economics of Transportation*, 4(4):241–255.
- Fosgerau, M. and Kim, J. (2019). Commuting and land use in a city with bottlenecks: Theory and evidence. *Regional Science and Urban Economics*, 77:182–204.
- Fosgerau, M., Kim, J., and Ranjan, A. (2018). Vickrey meets alonso: Commute scheduling and congestion in a monocentric city. *Journal of Urban Economics*, 105:40–53.
- Fosgerau, M. and Small, K. A. (2013). Hypercongestion in downtown metropolis. *Journal of Urban Economics*, 76:122–134.
- Fu, H., Chen, S., Chen, K., Kouvelas, A., and Geroliminis, N. (2021). Perimeter control and route guidance of multi-region mfd systems with boundary queues using colored petri nets. *IEEE Transactions on Intelligent Transportation Systems*, 23(8):12977–12999.
- Fujita, M. (1989). Urban economic theory. *Cambridge Books*.

- Genser, A. and Kouvelas, A. (2022). Dynamic optimal congestion pricing in multi-region urban networks by application of a multi-layer-neural network. *Transportation Research Part C: Emerging Technologies*, 134:103485.
- Geroliminis, N. (2015). Cruising-for-parking in congested cities with an mfd representation. *Economics of Transportation*, 4(3):156–165.
- Geroliminis, N. and Daganzo, C. F. (2008). Existence of urban-scale macroscopic fundamental diagrams: Some experimental findings. *Transportation Research Part B: Methodological*, 42(9):759–770.
- Geroliminis, N., Haddad, J., and Ramezani, M. (2012). Optimal perimeter control for two urban regions with macroscopic fundamental diagrams: A model predictive approach. *IEEE Transactions on Intelligent Transportation Systems*, 14(1):348–359.
- Geroliminis, N. and Levinson, D. M. (2009). Cordon pricing consistent with the physics of overcrowding. In *Transportation and Traffic Theory 2009: Golden Jubilee*, pages 219–240. Springer.
- Godfrey, J. (1969). The mechanism of a road network. *Traffic Engineering & Control*, 8(8).
- Gonzales, E. J. (2015). Coordinated pricing for cars and transit in cities with hypercongestion. *Economics of Transportation*, 4(1-2):64–81.
- Gonzales, E. J. and Daganzo, C. F. (2012). Morning commute with competing modes and distributed demand: user equilibrium, system optimum, and pricing. *Transportation Research Part B: Methodological*, 46(10):1519–1534.
- Gubins, S. and Verhoef, E. T. (2014). Dynamic bottleneck congestion and residential land use in the monocentric city. *Journal of Urban Economics*, 80:51–61.
- Guo, Q. and Ban, X. J. (2020). Macroscopic fundamental diagram based perimeter control considering dynamic user equilibrium. *Transportation Research Part B: Methodological*, 136:87–109.
- Haddad, J. (2017). Optimal perimeter control synthesis for two urban regions with aggregate boundary queue dynamics. *Transportation Research Part B: Methodological*, 96:1–25.
- Haddad, J. and Geroliminis, N. (2012). On the stability of traffic perimeter control in two-region urban cities. *Transportation Research Part B: Methodological*, 46(9):1159–1176.
- Haddad, J. and Shraiber, A. (2014). Robust perimeter control design for an urban region. *Transportation Research Part B: Methodological*, 68:315–332.
- Haddad, J. and Zheng, Z. (2020). Adaptive perimeter control for multi-region accumulation-based models with state delays. *Transportation Research Part B: Methodological*, 137:133–153.
- Haitao, H., Yang, K., Liang, H., Menendez, M., and Guler, S. I. (2019). Providing public transport priority in the perimeter of urban networks: A bimodal strategy. *Transportation Research Part C: Emerging Technologies*, 107:171–192.
- Hall, J. D. (2018). Pareto improvements from lexis lanes: The effects of pricing a portion of the lanes on congested highways. *Journal of Public Economics*, 158:113–125.
- Huang, Y., Ye, Y., Sun, J., and Tian, Y. (2023). Characterizing the impact of autonomous vehicles on macroscopic fundamental diagrams. *IEEE Transactions on Intelligent Transportation Systems*.

- Ji, Y. and Geroliminis, N. (2012). On the spatial partitioning of urban transportation networks. *Transportation Research Part B: Methodological*, 46(10):1639–1656.
- Jin, W.-L. (2020). Generalized bathtub model of network trip flows. *Transportation Research Part B: Methodological*, 136:138–157.
- Kanemoto, Y. (1980). Theories of urban externalities. *North-Holland*.
- Kolarova, V. and Cherchi, E. (2021). Impact of trust and travel experiences on the value of travel time savings for autonomous driving. *Transportation Research Part C: Emerging Technologies*, 131:103354.
- Kouvelas, A., Saeedmanesh, M., and Geroliminis, N. (2023). A linear-parameter-varying formulation for model predictive perimeter control in multi-region mfd urban networks. *Transportation Science*.
- Lamotte, R., De Palma, A., and Geroliminis, N. (2017). On the use of reservation-based autonomous vehicles for demand management. *Transportation Research Part B: Methodological*, 99:205–227.
- Lamotte, R. and Geroliminis, N. (2018). The morning commute in urban areas with heterogeneous trip lengths. *Transportation Research Part B: Methodological*, 117:794–810.
- Leclercq, L., Chiabaut, N., and Trinquier, B. (2014). Macroscopic fundamental diagrams: A cross-comparison of estimation methods. *Transportation Research Part B: Methodological*, 62:1–12.
- Li, Y., Mohajerpoor, R., and Ramezani, M. (2021). Perimeter control with real-time location-varying cordon. *Transportation Research Part B: Methodological*, 150:101–120.
- Li, Z.-C., Yu, D.-P., and de Palma, A. (2023). An analytical model for residential location choices of heterogeneous households in a monocentric city with stochastic bottleneck congestion. *THEMA Working Papers*, 2023-01.
- Liu, W. and Geroliminis, N. (2016). Modeling the morning commute for urban networks with cruising-for-parking: An mfd approach. *Transportation Research Part B: Methodological*, 93:470–494.
- Loder, A., Ambühl, L., Menendez, M., and Axhausen, K. W. (2019). Understanding traffic capacity of urban networks. *Scientific reports*, 9(1):1–10.
- Lu, Q., Tettamanti, T., Hörcher, D., and Varga, I. (2020). The impact of autonomous vehicles on urban traffic network capacity: an experimental analysis by microscopic traffic simulation. *Transportation Letters*, 12(8):540–549.
- Mariotte, G., Leclercq, L., and Laval, J. A. (2017). Macroscopic urban dynamics: Analytical and numerical comparisons of existing models. *Transportation Research Part B: Methodological*, 101:245–267.
- Moshahedi, N. and Kattan, L. (2022). A macroscopic dynamic network loading model using variational theory in a connected and autonomous vehicle environment. *Transportation research part C: emerging technologies*, 145:103911.
- Ni, W. and Cassidy, M. (2020). City-wide traffic control: modeling impacts of cordon queues. *Transportation research part C: emerging technologies*, 113:164–175.
- Ortigosa, J., Menendez, M., and Tapia, H. (2015). Study on the number and location of measurement points for an mfd perimeter control scheme: a case study of zurich. *EURO Journal on Transportation and Logistics*, 3(3):245–266.

- Ramezani, M., Haddad, J., and Geroliminis, N. (2015). Dynamics of heterogeneity in urban networks: aggregated traffic modeling and hierarchical control. *Transportation Research Part B: Methodological*, 74:1–19.
- Simoni, M. D., Pel, A. J., Waraich, R. A., and Hoogendoorn, S. P. (2015). Marginal cost congestion pricing based on the network fundamental diagram. *Transportation Research Part C: Emerging Technologies*, 56:221–238.
- Sirmatel, I. I. and Geroliminis, N. (2017). Economic model predictive control of large-scale urban road networks via perimeter control and regional route guidance. *IEEE Transactions on Intelligent Transportation Systems*, 19(4):1112–1121.
- Sirmatel, I. I., Tsitsokas, D., Kouvelas, A., and Geroliminis, N. (2021). Modeling, estimation, and control in large-scale urban road networks with remaining travel distance dynamics. *Transportation Research Part C: Emerging Technologies*, 128:103157.
- Small, K. A. and Chu, X. (2003). Hypercongestion. *Journal of Transport Economics and Policy (JTPE)*, 37(3):319–352.
- Steck, F., Kolarova, V., Bahamonde-Birke, F., Trommer, S., and Lenz, B. (2018). How autonomous driving may affect the value of travel time savings for commuting. *Transportation research record*, 2672(46):11–20.
- Takayama, Y. (2020). Who gains and who loses from congestion pricing in a monocentric city with a bottleneck? *Economics of Transportation*, 24:100189.
- Takayama, Y. and Kuwahara, M. (2017). Bottleneck congestion and residential location of heterogeneous commuters. *Journal of Urban Economics*, 100:65–79.
- Takayama, Y. and Kuwahara, M. (2020). Scheduling preferences, parking competition, and bottleneck congestion: A model of trip timing and parking location choices by heterogeneous commuters. *Transportation Research Part C: Emerging Technologies*, 117:102677.
- Tsekeris, T. and Geroliminis, N. (2013). City size, network structure and traffic congestion. *Journal of Urban Economics*, 76:1–14.
- van den Berg, V. A. and Verhoef, E. T. (2016). Autonomous cars and dynamic bottleneck congestion: The effects on capacity, value of time and preference heterogeneity. *Transportation Research Part B: Methodological*, 94:43–60.
- Vickrey, W. (2020). Congestion in midtown manhattan in relation to marginal cost pricing. *Economics of Transportation*, 21:100152.
- Wu, S. and Li, Z.-C. (2023). Managing a bi-modal bottleneck system with manned and autonomous vehicles: Incorporating the effects of in-vehicle activity utilities. *Transportation Research Part C: Emerging Technologies*, 152:104179.
- Xu, S.-X., Liu, R., Liu, T.-L., and Huang, H.-J. (2018). Pareto-improving policies for an idealized two-zone city served by two congestible modes. *Transportation Research Part B: Methodological*, 117:876–891.
- Yildirimoglu, M., Ramezani, M., and Geroliminis, N. (2015). Equilibrium analysis and route guidance in large-scale networks with mfd dynamics. *Transportation Research Part C*, 59:404–420.

- Yildirimoglu, M., Sirmatel, I. I., and Geroliminis, N. (2018). Hierarchical control of heterogeneous large-scale urban road networks via path assignment and regional route guidance. *Transportation Research Part B: Methodological*, 118:106–123.
- Zheng, N., Dantsuji, T., Wang, P., and Geroliminis, N. (2017). Macroscopic approach for optimizing road space allocation of bus lanes in multimodal urban networks through simulation analysis. *Transportation Research Record*, 2651(1):42–51.
- Zheng, N. and Geroliminis, N. (2013). On the distribution of urban road space for multimodal congested networks. *Transportation Research Part B: Methodological*, 57(C):326–341.
- Zheng, N., Waraich, R. A., Axhausen, K. W., and Geroliminis, N. (2012). A dynamic cordon pricing scheme combining the macroscopic fundamental diagram and an agent-based traffic model. *Transportation Research Part A: Policy and Practice*, 46(8):1291–1303.
- Zhong, H., Li, W., Burris, M. W., Talebpour, A., and Sinha, K. C. (2020). Will autonomous vehicles change auto commuters’ value of travel time? *Transportation Research Part D: Transport and Environment*, 83:102303.
- Zhou, D. and Gayah, V. V. (2023). Scalable multi-region perimeter metering control for urban networks: A multi-agent deep reinforcement learning approach. *Transportation Research Part C: Emerging Technologies*, 148:104033.